Reviewed research article

Geomorphologic evidence of jökulhlaups along the Hvítá river, southwestern Iceland

Greta H. Wells[1,2,3], Andrew J. Dugmore[3,4], Þorsteinn Sæmundsson[2,5], Timothy Beach[1], Sheryl Luzzadder-Beach[1] and Daniel Ben-Yehoshua[6]

[1]*Department of Geography and the Environment, University of Texas at Austin*

[2]*Institute of Earth Sciences, University of Iceland*

[3]*School of Geosciences, University of Edinburgh*

[4]*Graduate Center, City University of New York*

[5]*Faculty of Life and Environmental Sciences, University of Iceland*

[6]*Faculty of Civil and Environmental Engineering, University of Iceland*

Corresponding author ghwells@hi.is; https://doi.org/10.33799/jokull2022.72.035

Abstract — *Glacial outburst floods (jökulhlaups) have been a significant driver of landscape evolution and environmental change throughout the Quaternary. Iceland experiences more frequent jökulhlaups than nearly anywhere else on Earth, though most research focuses on subglacial volcanogenic floods that drain across outwash plains. Abundant geomorphologic evidence exists for large-scale jökulhlaups that drained along the modern-day course of the Hvítá river in southwestern Iceland during early Holocene deglaciation, originating from ice-dammed Kjölur glacial lake; yet only one previous publication has investigated these events. This study uses a combination of field mapping and remote sensing to identify new jökulhlaup geomorphologic evidence along the Hvítá river, including erosional landforms such as scoured bedrock, anastomosing channel networks, cataracts, and canyons, and depositional features such as boulder bars and channel infill. We synthesize new findings with previously reported work to: 1) present an updated geomorphologic map of Hvítá jökulhlaup evidence; 2) reconstruct flood drainage routes, landscape impact, hydrology, and relative chronology; and 3) hypothesize scenarios of ice margin position and glacial lake evolution. Interpreting flood landform assemblages reveals a more extensive geomorphologic record than previously reported, with a complex drainage pattern along four separate routes from two potentially different sources. Reconstructed peak flow discharges span three orders of magnitude from 10^2 to 10^5 m^3s^{-1}. Geomorphologic and paleohydraulic results introduce four hypothesized drainage scenarios, though absolute geochronology is necessary to determine whether multiple floods drained along each route. The Hvítá jökulhlaups yield insight into the timing and dynamics of the final phase of Icelandic Ice Sheet decay, advancing understanding of Iceland's Pleistocene–Holocene transition, demonstrating the importance of high magnitude, low frequency floods in landscape evolution, and serving as an analogue to ice and meltwater response to past, present, and future climate warming in glaciated regions worldwide.*

INTRODUCTION AND AIMS

Glacial outburst floods (jökulhlaups) have occurred throughout the Quaternary as well as earlier glacial periods and are a significant contemporary geohazard in glaciated regions worldwide (Baker, 2013; Carrivick and Tweed, 2016; Harrison *et al.*, 2018; Wells *et al.*, 2022). These sudden, rapid drainages of glacial meltwater can erode bedrock, redistribute sediment, and restructure hydrologic networks on both local and regional scales, creating geomorphic legacies that may persist in the environmental record (Carling, 2013; Jacquet *et al.*, 2017; Cook *et al.*, 2018; Piret *et al.*, 2022). At their largest, they may also disrupt ocean circulation patterns to influence global climate (Clarke *et al.*, 2004; Praetorius *et al.*, 2020; Brovkin *et al.*, 2021).

Iceland experiences jökulhlaups more frequently than nearly anywhere else on Earth. Research has focused on the most commonly occurring events, which are triggered by subglacial volcanic or geothermal activity beneath ice caps and generally drain across sandurs (glacial outwash plains) (Tómasson, 1996; Maizels, 1997; Björnsson, 2002; Carrivick *et al.*, 2004b; Roberts, 2005; Russell *et al.*, 2005; Rushmer, 2006; Russell *et al.*, 2006; Marren *et al.*, 2009; Dunning *et al.*, 2013; Magnússon *et al.*, 2021). Comparatively few studies have investigated non-volcanogenic Icelandic jökulhlaups, with research limited to historical floods from ice-marginal lakes (Thorarinsson, 1939; Roberts *et al.*, 2005; Þorsteinsson *et al.*, 2021), ice-marginal lake drainage during early Holocene deglaciation in northeastern and central Iceland (Tómasson, 1993; Van Vliet-Lanoë *et al.*, 2020), and a jökulhlaup triggered by a rockfall at the Steinsholtsjökull glacier and proglacial lake in 1967 (Kjartansson, 1967). There is also a relative dearth of research on Icelandic jökulhlaup geomorphologic impact in bedrock terrain, with existing publications generally focused on the Jökulsá á Fjöllum river in northeastern Iceland (Tómasson, 1973; Russell *et al.*, 2005; Baynes *et al.*, 2015a, 2015b; Carrivick and Tweed, 2019) but with some work in central Iceland (Tómasson, 1993). However, jökulhlaups from ice-marginal lakes in bedrock settings may be more representative of most global glacial outburst floods and might have been more typical of activity during the decay of the last Icelandic Ice Sheet (IIS) (Komatsu *et al.*, 2016; Benito and Thorndycraft, 2020; Fisher, 2020; O'Connor *et al.*, 2020).

Abundant evidence exists in Iceland for jökulhlaups that drained from ice-dammed lakes during late Pleistocene-early Holocene deglaciation. Some of the most prominent jökulhlaup landforms occur along the modern-day course of the Hvítá river in southwestern Iceland, formed by floods from ice-dammed Glacial Lake Kjölur; yet only one publication has investigated these events (Tómasson, 1993). Our study reports new geomorphologic evidence and synthesizes previous work to: 1) present an updated geomorphologic map of Hvítá jökulhlaup evidence; 2) reconstruct flood drainage routes, landscape impact, hydrology, and relative chronology; and 3) hypothesize scenarios of ice margin position and glacial lake evolution during early Holocene deglaciation. Results have advanced understanding of the final phase of ice sheet retreat and provided useful insight into jökulhlaup processes and geomorphologic impacts in glaciated regions worldwide.

STUDY AREA

The Kjölur region is situated in the western part of the central highlands between the current Langjökull and Hofsjökull ice caps, occupying a plateau ∼400–700 meters above sea level (m asl) that is punctuated by tuyas (subglacially-erupted table mountains) (Figure 1) (Kjartansson, 1964; Tómasson, 1993). Today, this sparsely vegetated area contains abundant evidence of glacial activity, widely overlain with aeolian sands and a poorly sorted cobble-gravel mélange mechanically weathered from glacial deposits (Áskelsson, 1946; Kjartansson, 1964; Kaldal and Víkingsson, 1990; Tómasson, 1993). Bedrock is dominated by tholeiitic basalt erupted during late Pleistocene interglacial/interstadial periods (younger than 0.8 million years ago (mya)) and also contains two early Holocene lava flows, the Kjalhraun and the Leggjabrjótur lava (Figure 1) (Sinton *et al.*, 2005; Jóhannesson and Sæmundsson, 2009; Eason *et al.*, 2015). The southern part of Kjölur includes Hvítárvatn, a 29 km^2 proglacial lake and source of the Hvítá river, which flows south to the Atlantic Ocean (Larsen *et al.*, 2012). Jökulhlaup evidence is most prominent along a ∼30 km-long reach near the Hvítá river between the Bláfell tuya and the Hvítárgljúfur canyon.

PALEOENVIRONMENTAL CONTEXT AND PREVIOUS RESEARCH

At the Last Glacial Maximum, roughly 25,000 calendar years before present (25 ka), Iceland was covered by an ice sheet 1000–2000 m thick at its center that extended beyond the present coastline (Hubbard *et al.*, 2006; Patton *et al.*, 2017). During the last glacial-

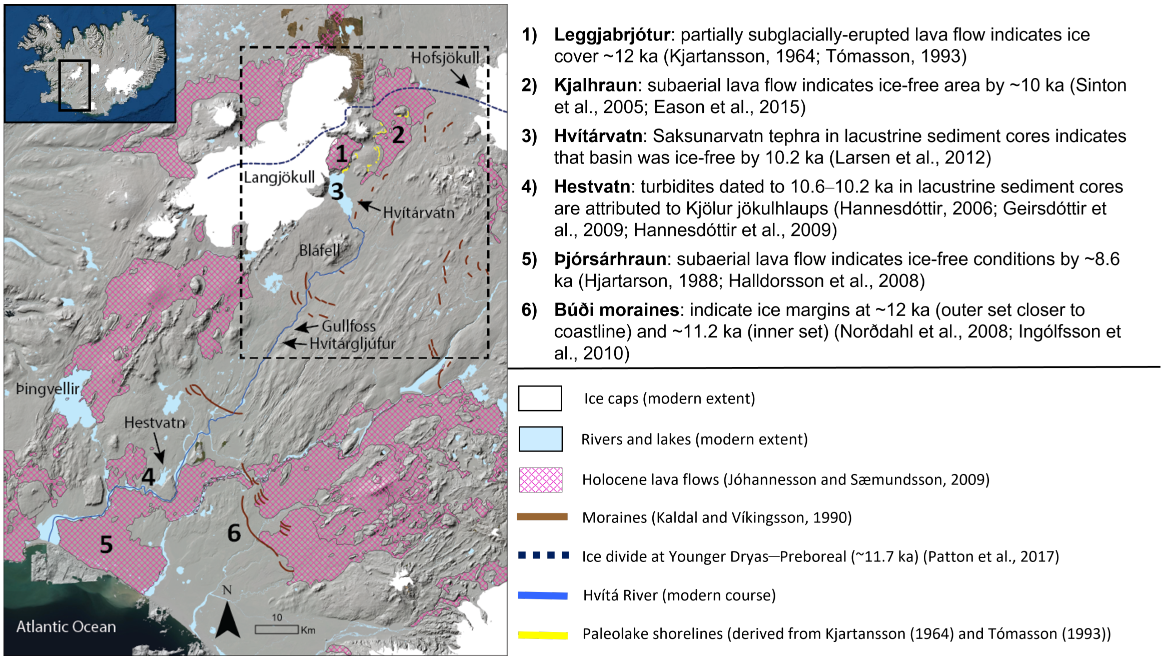

Figure 1. Overview map of paleoenvironmental evidence of ice marginal positions, glacial lake shorelines, and Holocene lavas along the Hvítá river from Kjölur to the Atlantic Ocean. Black dotted box denotes the study area shown in Figure 2. ArcticDEM basemap (Porter *et al.*, 2018). – *Ummerki fornra jökuljaðra, jökullóna og strandlína ásamt útlínum nútímahrauna umhverfis farveg Hvítár, frá Kili til sjávar. Svarti ramminn afmarkar rannsóknarsvæðið á 2. mynd. Grunnkortið er byggt á ArcticDEM hæðarlíkani Porter o.fl. (2018).*

interglacial transition, the IIS began a rapid stepwise retreat interrupted by glacial readvances in the Younger Dryas (∼12 ka) and Preboreal (∼11.2 ka), which formed the Búði moraines in southwestern Iceland (Norðdahl *et al.*, 2008; Ingólfsson *et al.*, 2010). As a result of rapid warming during the Holocene Thermal Maximum, ice extent was probably equivalent to, or less than, modern-day cover by 8.7 ka (Geirsdóttir *et al.*, 2009; Axford *et al.*, 2021). The timing and pattern of this final phase of deglaciation, however, remains poorly constrained, with few paleoenvironmental records, particularly in the central highlands (Figure 1) (Norðdahl *et al.*, 2008; Ingólfsson *et al.*, 2010; Patton *et al.*, 2017; Andrés *et al.*, 2019).

A handful of studies have investigated IIS retreat, glacial lake formation, and jökulhlaup drainage in the Kjölur region. Áskelsson (1946) hypothesized that glaciofluvial sediments on the eastern margin of Kjölur were deposited in a delta within an ice-contact lake. Kjartansson (1964) and Tómasson (1993) subsequently mapped paleolake shoreline locations and elevations on tuyas to estimate stages of ice-dammed Glacial Lake Kjölur (Figure 1). Tómasson (1993; 2002) hypothesized that the lake filled to a maximum volume of 25–30 km^3 and drained approximately every decade over a period of 100–200 years as a result of ice dam failure at three outlets, which shifted according to lake surface elevation, ice margin position, and ice divide location. Synthesizing shoreline positions, geomorphologic evidence, and paleohydraulic estimates from flood channel cross sections, Tómasson (1993; 2002) proposed that the first jökulhlaups drained north, reaching a maximum peak discharge of 40,000 m^{3}s^{-1} (Figure 2A); the second group drained south on the western side of Bláfell with a peak discharge of 20,000 m^{3}s^{-1} (Figure 2B); and the final set drained east of Bláfell, reaching 200–

300,000 m^3s^{-1} (Figure 2C). Tómasson (1993) dated these events around 9500 ^{14}C yr BP, a few hundred years after Preboreal Búði moraine formation, based on radiocarbon dates of the moraines.

METHODS

Geomorphologic mapping was conducted using a combination of field surveys and remote sensing. A topographic digital elevation model (ÍslandsDEM, 2021), satellite imagery (Google Earth), and aerial photographs (Landmælingar Íslands; Loftmyndir ehf.) were used to map features >10 m resolution, while field surveys were necessary to identify small-scale landforms (<10 m) and ground truth and interpret geomorphologic context. Jökulhlaup landforms were identified based on criteria developed in flood landscapes worldwide, particularly in analogue basalt terrain (i.e. Bretz, 1923; Baker, 1973, 2009; O'Connor, 1993; Rathburn, 1993; Carrivick *et al.*, 2004a; Herget, 2005; Russell *et al.*, 2005; Baynes *et al.*, 2015a). Geomorphologic evidence was subsequently interpreted using the methodology and conceptual framework described in Wells *et al.* (2022). Glacial features were identified and described according to criteria in Glasser and Bennett (2004), Bennett and Glasser (2009), and Benn and Evans (2010).

Landform geographic coordinates and elevations were recorded with a Garmin 64s handheld GPS (±3 m accuracy). Feature dimensions were measured with a tape measure, where applicable, and glacial striation orientation was measured using a compass. GPS points were then imported into ArcGIS Pro (version 2.6.0) and converted into polygons to create a geomorphologic map of the study area with a topographic digital elevation model basemap (ÍslandsDEM, 2021). Two areas, the Kórgil and Hvítárgljúfur canyons, were also mapped with a drone-mounted camera (DJI Mavic 2Pro) to collect high-resolution imagery for Structure-from-Motion (SfM), which was processed with Pix4D Mapper and analyzed with CloudCompare (open-source software) to generate centimeter-scale, two- and three-dimensional data of the canyons (ground sampling distance = 5 cm; drone-mounted GPS accuracy ± 5 m horizontal and 10 m vertical). A qualitative comparison of the produced orthomosaic showed only a minimal offset from georeferenced aerial imagery provided by Loftmyndir ehf. (within 1 m). For the purposes of this study, a more accurate georeferencing was not necessary. The results of the drone surveys are high-resolution elevation models, orthomosaics, colored point clouds, and 3D-meshes for analysis and correction of errors generated by shadow effects in the mentioned datasets.

We reconstructed jökulhlaup hydrology using boulder paleocompetence and Manning's equation. For paleocompetence, we measured the 6–10 largest boulders at each site and determined the largest clast by summing triaxial dimensions (long + middle + short axes). We used these input values along with parameters and equations from Baynes *et al.* (2015a) and Stokes *et al.* (2012) to calculate the minimum hydraulic conditions required to transport the largest boulder at each site. For Manning's equation, we used equations in Ward and Trimble (2004) to estimate peak flow discharge at channel cross sections. We held Manning's n constant at 0.04 based on field observations of modern surface cover (Chow, 1959). For both methods, channel cross-sectional dimensions were approximated from a drone-mapped SfM topographic model (for profiles at the Grjótá channel, Kórgil canyons, and Hvítárgljúfur) or ÍslandsDEM (2021) (for profiles at the Grjótá valley, Hvítá river, eastern Gullfoss, and Sandá channels). Bed slope was derived from transects perpendicular to cross sections but outside of channels to reduce inaccuracies from channel infill elevations.

RESULTS: GEOMORPHOLOGICAL EVIDENCE BETWEEN BLÁFELL AND HVÍTÁRGLJÚFUR

Glacial and glaciofluvial evidence

The area between Bláfell and Hvítárgljúfur is typified by glaciated landscapes–landforms of glacial erosion and deglaciation mantled by a poorly sorted cobble-gravel mélange with occasional boulders and degraded by limited amounts of paraglacial transformation. Prominent glacial features include striated bedrock outcrops, erratic boulders up to ∼4 m diameter, till exposures, and whaleback streamlined bedrock

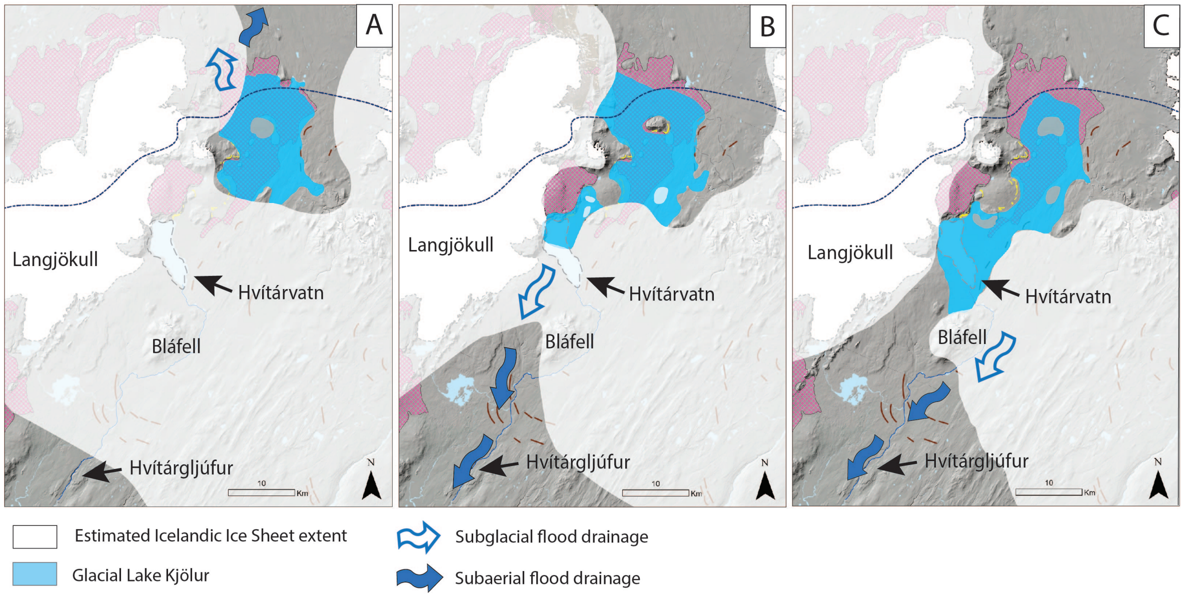

Figure 2. Study area with estimated ice sheet position, glacial lake extent, and jökulhlaup drainage routes based on Tómasson (1993). See Figure 1 for basemap key. – *Áætluð lega jökla, umfang jökullóna og farvega jökulhlaupanna á rannsóknarsvæðinu samkvæmt niðurstöðum Hauks Tómassonar (1993). Sjá skýringar á 1. mynd.*

forms that often exhibit striated or plucked surfaces. Glaciofluvial sediments outcrop in three locations, providing evidence for extensive proglacial meltwater drainage. The most frequent fluvioglacial exposures occur in gravel-mantled hills at the southwestern base of Bláfell, consisting of cm-to-m-scale layers of sand, gravel, and cobbles, resembling those in modern Icelandic sandurs and affected by periods of variable flow energy in proglacial rivers (Maizels, 1997; Marren, 2002, 2005; Bennett and Glasser, 2009; Benn and Evans, 2010). Additional striations and moraines were previously mapped in the study area by Kjartansson (1964), Kaldal and Víkingsson (1990), and Tómasson (1993) (Figure 3).

Jökulhlaup evidence

Jökulhlaup evidence is imprinted over this glacial landscape along a ∼30 km-long reach between Bláfell and Hvítárgljúfur. Tómasson (1993) mapped some of these features, namely anastomosing bedrock channels, cataracts, and canyons on the western side of Bláfell; boulder deposits in the Grjótá valley; gravel bars along the Hvítá river; and cataracts, canyons, and strath terraces at Hvítárgljúfur. We extended this mapping and provide additional jökulhlaup evidence not previously reported. Our geomorphologic evidence is organized into four sections based on geographic location (Figure 3). Additionally, Tómasson (1993) identified flood-eroded bedrock channels on the southeastern side of Bláfell. However, the Hvítá's western bank at this location displays no definitive flood or glacial evidence, and we have not yet carried out field surveys on the eastern bank to confirm flood provenance. Thus, we use remote sensing imagery to map these as potential channels.

Western Bláfell

The first area of jökulhlaup evidence occurs on the western side of Bláfell (Figure 4). A series of anastomosing bedrock channels slopes south from the Bláfellsháls saddle to the Grjótá valley covering an area up to ∼4 km long and ∼3.5 km wide and dropping ∼300 m vertically. These channels are cut into smoothed hills mantled with a poorly sorted mélange of gravel, cobbles, and small boulders firmly anchored with moss. Channels begin as dry, shallow linear depressions filled with angular, moss-anchored boulders (0.25–0.75 m diameter) (Figure 4.1).

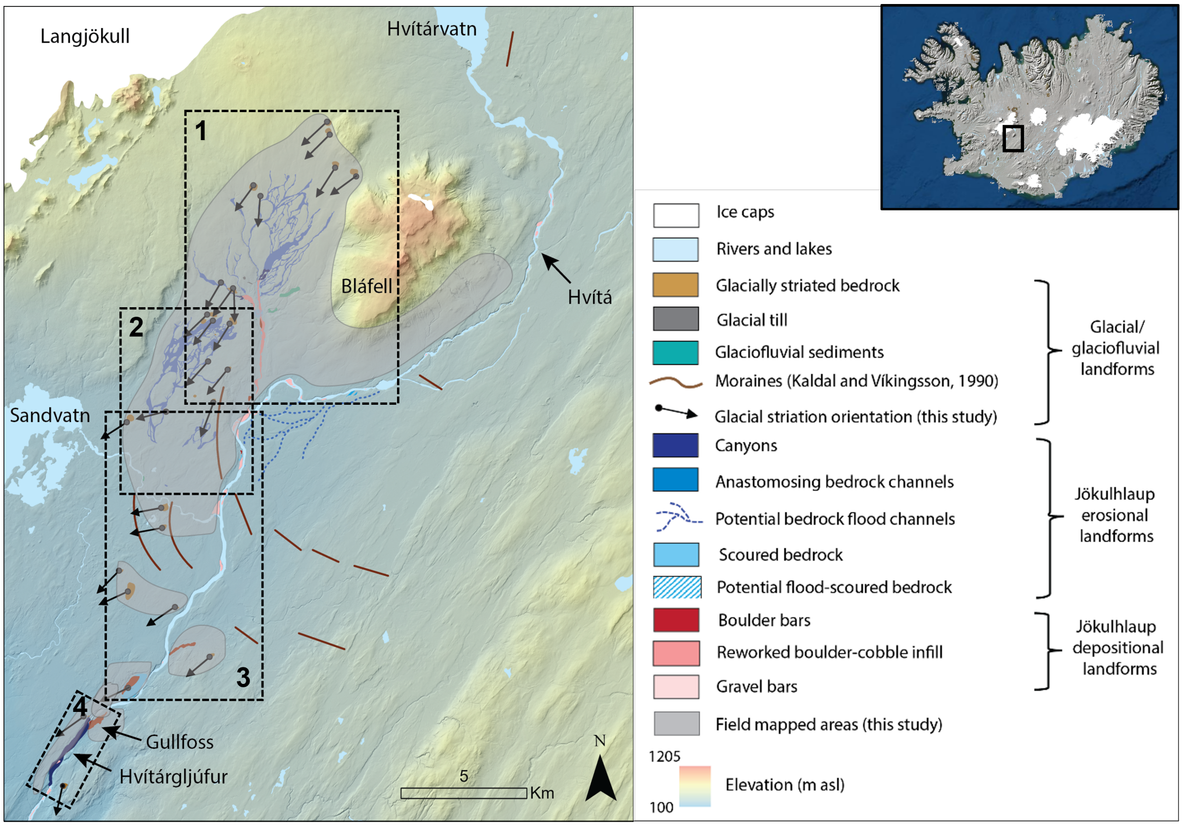

Figure 3. Survey area showing the geomorphologic evidence mapped in this study. Black dotted boxes denote four subregions: 1) western Bláfell (Figure 4); 2) Sandá channels (Figure 8); 3) Hvítá river (Figure 10); 4) Gullfoss waterfall and Hvítárgljúfur canyon (Figure 11). ÍslandsDEM (2021) basemap. – *Landfræðileg ummerki sem voru kortlögð í þessu verkefni. Svartar punktalínan afmarkar fjögur rannsóknarsvæði: 1) Vestanvert Bláfell (4. mynd), 2) Farvegi við Sandá (8. mynd); Hvítá (10. mynd); Gullfoss og Hvítárgljúfur (11. mynd). Grunnkortið byggir á ÍslandsDEM (2021) hæðarlíkaninu.*

At 1.5 km south of Bláfellsháls, channels transition to an alternating sequence of four main features of jökulhlaup evidence (Figure 5). The first feature includes m-scale, scoured bedrock outcrops containing grooves and flutes mostly oriented parallel to downhill flow, potholes, and some angular slabs of fragmented bedrock (Figures 4.2 and 5.1). Feature 2 consists of <1 m high bedrock steps eroded along basalt bedding planes that progressively scale up to amphitheater-shaped cataracts opening downstream (Figures 4.3 and 5.2). The largest cataract occurs ∼3 km from the start of flood evidence and measures ∼120 m wide and ∼30 m deep. The third feature includes depressions (plunge pools) at cataract bases, infilled with relatively well-sorted, subangular cobbles and boulders (∼0.5–1 m diameter) that sometimes form a flat, compacted boulder pavement (Figure 5.3). Feature 4 consists of subangular to subrounded boulder deposits (∼1–2 m diameter) that extend downstream, often to the scoured bedrock outcrop at the start of the next sequence (Figure 5.4). Bedrock shows a strong lithological control, with massive outcrops (with no clear jointing patterns) displaying grooves, flutes, and potholes (Figure 5.1), while porphyritic basalt (with submeter scale columnar jointing) contains evidence of "short stack" columnar basalt fragmentation. Some

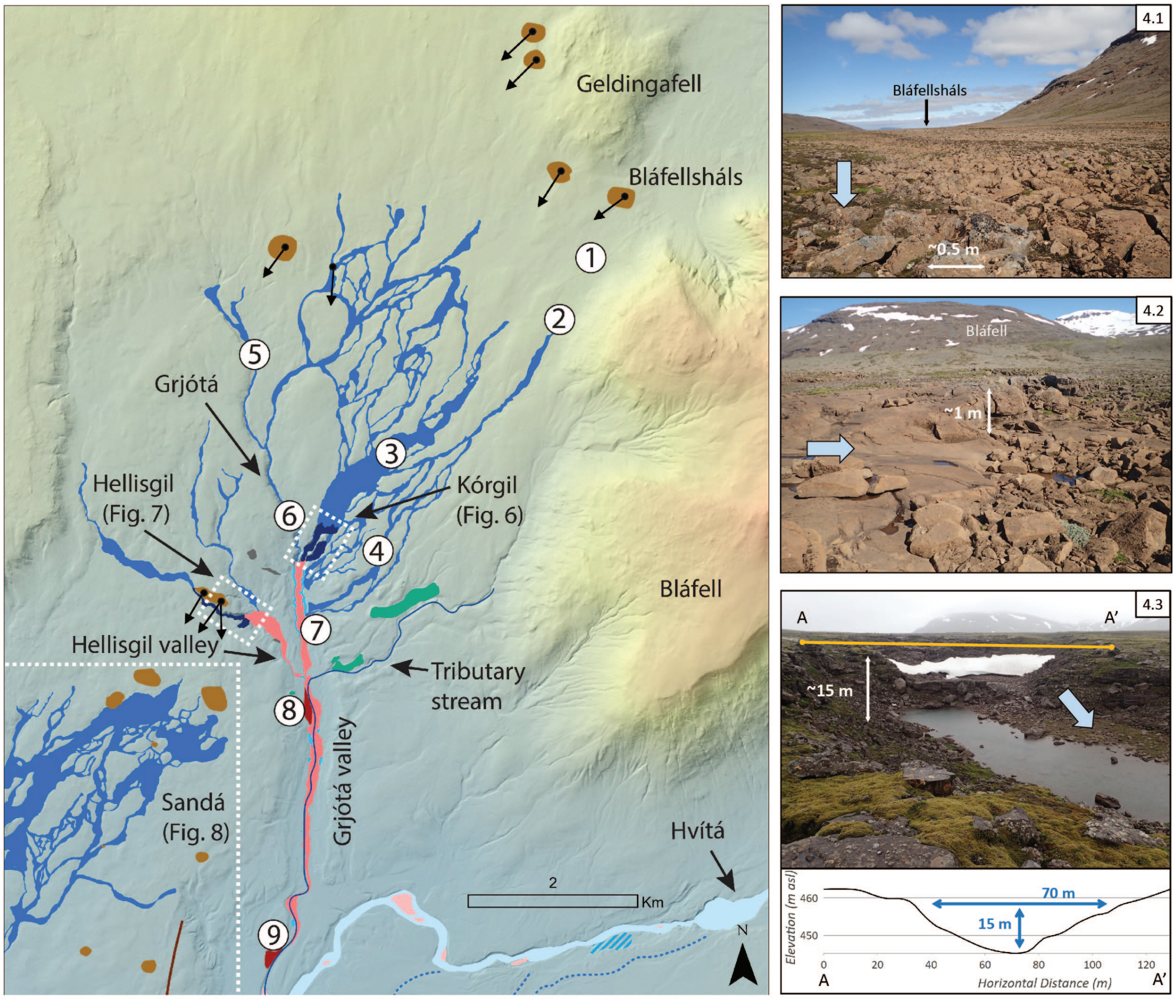

Figure 4. Geomorphologic map of the western Bláfell channels and examples of flood landforms and cross-sectional profiles. Numbers on map correspond to photo locations. Figures 4.4–4.9 are presented on the next page. Blue arrows in photos denote flood direction. Profile elevation data is from ÍslandsDEM (2021). See Figure 3 for map key. – *Landmótunarkort af vesturhluta farvega við Bláfell ásamt þversniðum og ljósmyndum af landformum sem mynduðust í jökulhlaupum. Tölur á kortinu samsvara staðsetningu ljósmyndanna. Myndir 4.4–4.9 eru á næstu blaðsíðu. Bláar örvar tákna flæðistefnu jökulhlaupanna. Grunnkortið og þversniðin eru byggð á ÍslandsDEM (2021) hæðarlíkaninu. Sjá skýringar á 3. mynd.*

boulders also display this columnar structure, and others contain pahoehoe textures similar to those on erosional basalt bedding planes (Figures 5.2 and 5.4) (Whipple *et al.*, 2000; Carrivick *et al.*, 2004a).

The largest-scale features occur in channels in the center of the network, with marginal channels continuously traceable in the field but containing smaller-scale landforms (Figure 4.4). Rocks within channels are typically weathered, lichened, and anchored with moss, though the central, lowest points of some channels contain polished, lichen-free surfaces, subrounded gravels and cobbles, and sand patches, indicating recent fluvial activity. The two westernmost channels in the anastomosing network display

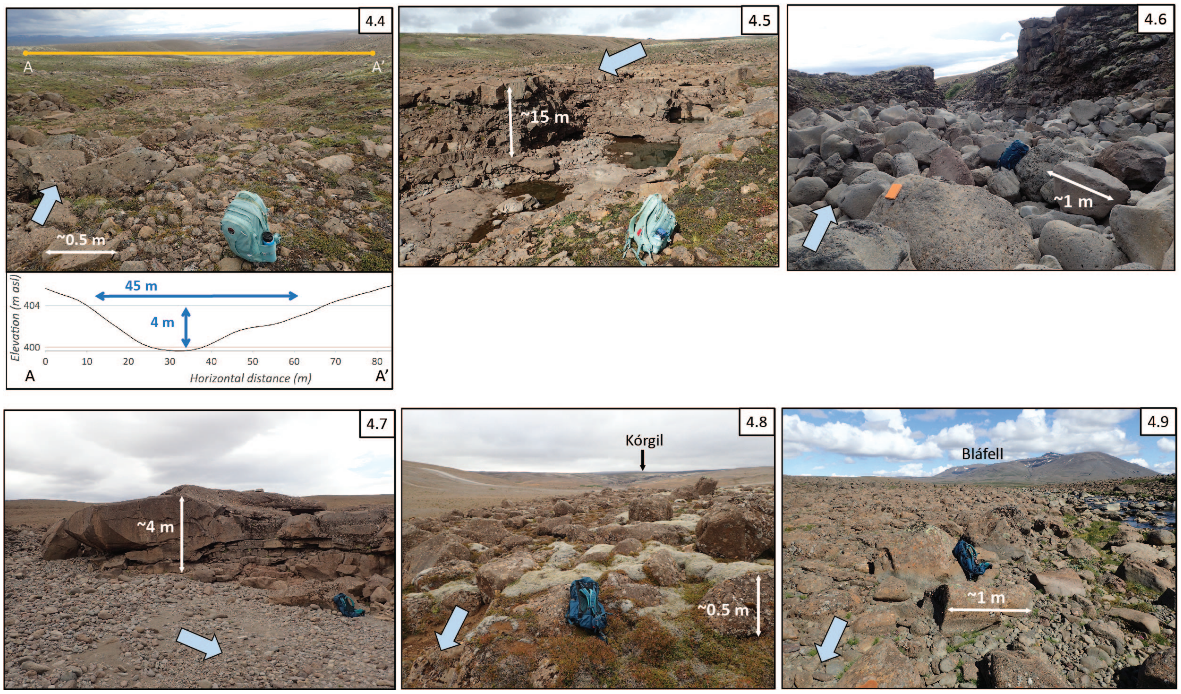

Figure 4. Cont. – *Framhald.*

signs of more intensive fluvial modification that spans the width of the channel, with polished, lichen-free bedrock, rounded gravel, sand deposits, and cataract rims with inset notches (Figure 4.5). These two channels merge into a single conduit (the Grjótá channel), the downstream-most few hundred meters of which is infilled with at least 2–3 m of subangular to subrounded, polished boulders up to 3 m in diameter (Figure 4.6).

About 4 km from Bláfellsháls, the largest, central channels coalesce into the Kórgil canyons, which have amphitheater-shaped cataracts at their upstream ends that are incised with bedrock notches connecting to channels in the anastomosing network (Figure 6). Canyon morphology closely resembles cataracts in analogue basalt landscapes, notably at the Ásbyrgi canyon, northeastern Iceland (Baynes *et al.*, 2015a, 2015b); Dry Falls, Channeled Scabland, Washington State, U.S.A. (Baker, 1973; Lehnigk and Larsen, 2022); Box Canyon, Big Lost River, Idaho, U.S.A. (Rathburn, 1993; Lamb *et al.*, 2008); and Malad Gorge, Idaho, U.S.A. (Lamb *et al.*, 2014). Canyon lithology is subaerially-erupted basalt with no uniform jointing pattern, and canyon walls are nearly vertical, though in most places their lower half is covered in grassy talus slopes. The northwestern canyon, Valagil ($\sim$550 m long, up to $\sim$125 m wide, and up to $\sim$70 m deep), contains weathered, lichened, angular to subangular boulders up to 2 m diameter, with smaller clasts infilling interstices (Figure 6c). The southeastern canyon, Kór ($\sim$300 m long, up to $\sim$110 m wide, and up to $\sim$60 m deep), is more circular, with talus sloping down to a flat, grassy floor studded with sporadic boulders (Figure 6b).

Synthesizing our geomorphologic evidence, we hypothesize a multi-stage process for Kórgil evolution (Figure 6). This hypothesized sequence of events would explain: 1) the morphologies of both canyons; 2) the directly aligned chute extending between the Valagil and Kór upstream notches (Figure 6a); 3) the presence of more boulders in Valagil than Kór; and 4) why Valagil displays more recent fluvial activity than

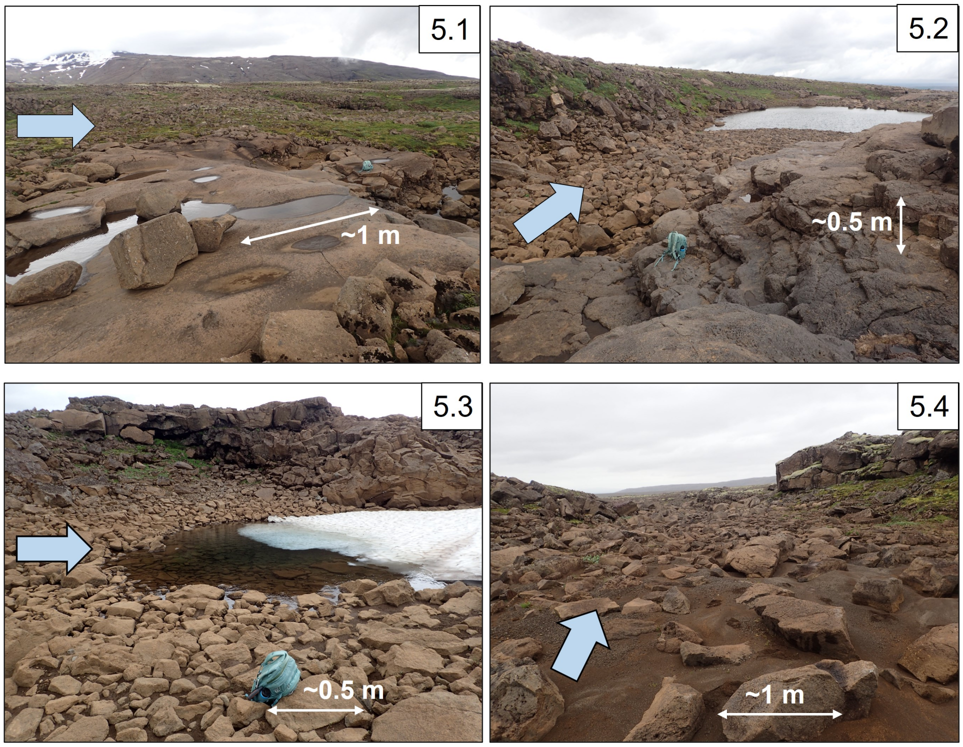

Figure 5. Sequence of geomorphologic features in the western Bláfell channels showing the progression from erosional to depositional landforms within a channel. Blue arrows indicate jökulhlaup flow direction. – *Vesturhluti farvega við Bláfell með ummerki rofs og setmyndunar úr jökulhlaupum. Bláar örvar sýna flæðistefnu hlaupanna.*

Kór. A similar process (i.e. a form of stream piracy indicated by a truncated cataract in a pair of parallel canyons) is observed with the Ástjörn and Ásbyrgi cataracts at the Jökulsárgljúfur canyon in northeastern Iceland (Baynes *et al.*, 2015a; van der Bilt *et al.*, 2021).

The western Bláfell anastomosing channels and Kórgil canyons end in the Grjótá valley, which continues for ∼4 km until its confluence with the Hvítá river (Figure 4). The valley margins contain bedrock features up to ∼5–10 m tall with bedrock steps and scoured upper surfaces, which decrease in height downstream and occasionally occur in the center of the channel (Figure 4.7). The valley is infilled with deposits up to 2–3 m thick (where visible) of subrounded to rounded, well-sorted, polished cobbles and boulders. Clast diameters fine downstream from ∼2–3 m where the Grjótá channel enters the valley to ∼0.3–1 m (∼1.5 m maximum) after ∼1 km and to ∼5–20 cm after ∼2 km. Recently active channels have dissected this infill, marked by smaller, more rounded, polished clasts and some sand and gravel, which also form backwater deposits at the entrance of Valagil. The valley has been dry at every observation except for a small, underfit tributary stream that enters from Bláfell and occupies the valley center until its confluence with the Hvítá.

The Grjótá valley also features a boulder bar (∼400 m long, up to 85 m wide, and up to 9 m high), oriented parallel to flow direction and composed of weathered, lichened, subangular to subrounded clasts up to 3.9 m diameter, with smaller boulders and cobbles infilling interstices (Figure 4.8). Another boulder bar occurs at the Hvítá confluence, oriented roughly parallel to Grjótá flow direction and composed of subrounded to subangular, well-sorted,

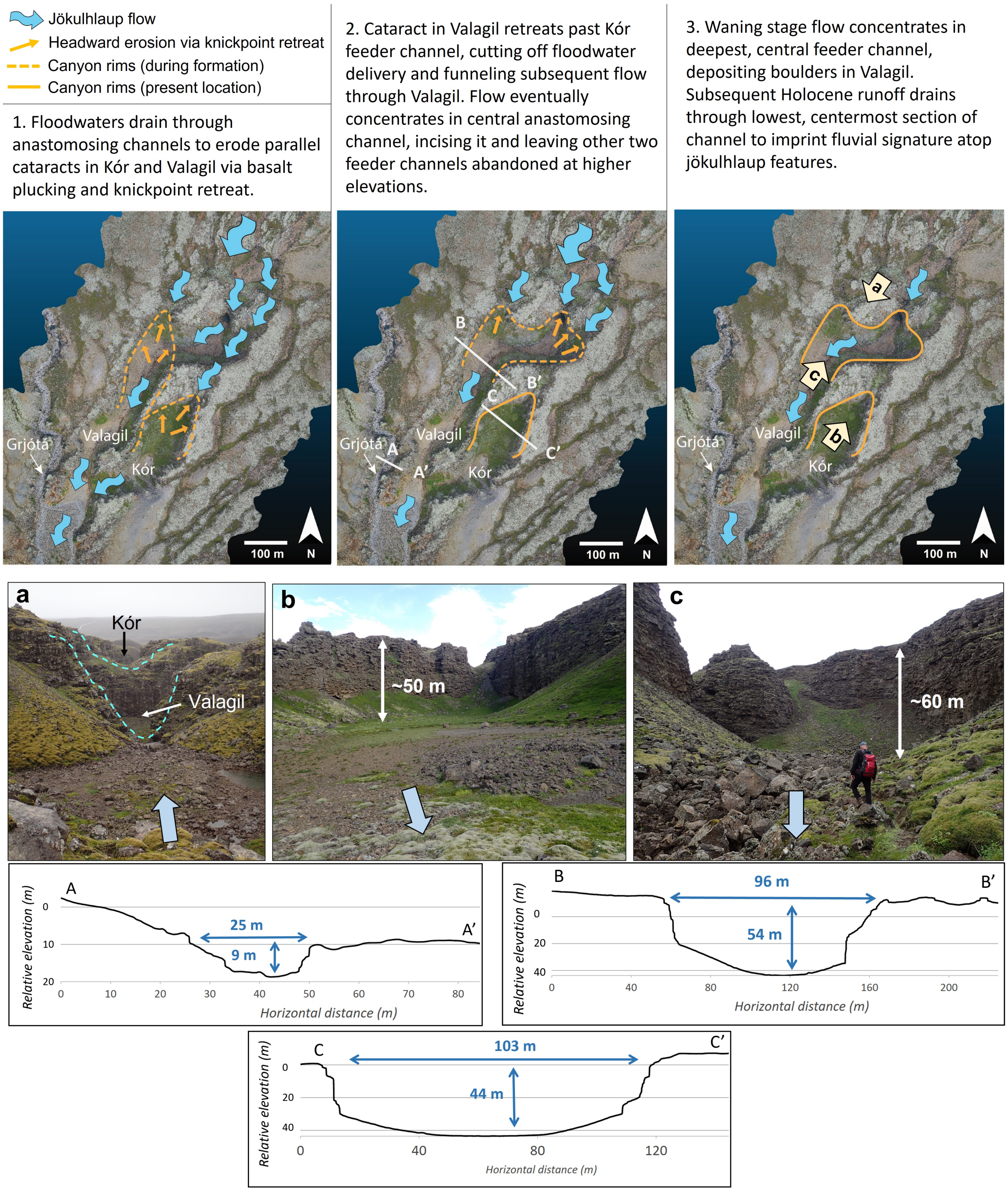
Jökulhlaup flow
Headward erosion via knickpoint retreat
Canyon rims (during formation)
Canyon rims (present location)
1. Floodwaters drain through anastomosing channels to erode parallel cataracts in Kór and Valagil via basalt plucking and knickpoint retreat.
2. Cataract in Valagil retreats past Kór feeder channel, cutting off floodwater delivery and funneling subsequent flow through Valagil. Flow eventually concentrates in central anastomosing channel, incising it and leaving other two feeder channels abandoned at higher elevations.
3. Waning stage flow concentrates in deepest, central feeder channel, depositing boulders in Valagil. Subsequent Holocene runoff drains through lowest, centermost section of channel to imprint fluvial signature atop jökulhlaup features.
Grjótá
Valagil
Kór
B
B'
C
C'
A
A'
a
b
c
100 m
N
Kór
Valagil
~50 m
~60 m
25 m
9 m
Relative elevation (m)
Horizontal distance (m)
96 m
54 m
103 m
44 m

maximum 2–3 m diameter boulders that fine to a cobble-gravel mix ~300 m downstream (Figure 4.9). An active stream incision indicates that boulder deposits are ~2–3 m thick.

Another valley, here called the Hellisgil valley, runs roughly parallel to the Grjótá and joins it after 1 km, separated by gently sloping terrain ~20–30 m high that is mantled by an unsorted cobble-gravel-small boulder mélange of an ambiguous provenance (Figure 4). This valley contains subrounded cobbles and small boulders and sporadic outcrops of scoured bedrock and is fed by a series of small, dry bedrock channels and a pair of canyons. The longer, narrower gorge, Hellisgil (~500 m long, up to ~85 m wide, and ~10–35 m deep), is box-shaped and contains a similar sequence of scoured bedrock, step cataracts, plunge pools, and boulder infill as the western Bláfell anastomosing channels, though sections also contain extensive talus slopes, indicative of mass wasting (Figure 7c). Rock surfaces in the center of the gorge are polished, rounded, and include cobble- and gravel-sized clasts and inset notches eroded into larger cataracts. The canyon's upper half is narrower, meandering, and more V-shaped. It continues upstream as a shallow gravel-cobble-small boulder-filled channel for 1.3 km, where it transitions into an incised bedrock channel with step cataracts up to ~15 m high whose floors contain polished, rounded boulder infill and sporadic observed flowing water.

An unnamed canyon occurs immediately south of Hellisgil (~115 m long, ~70 m wide, and ~30 m deep), ending in an amphitheater-shaped cataract with two distinct notches in its rim, one of which connects to Hellisgil via a faint, vegetated trough (Figure 7a). The cataract base is undercut, and the canyon contains a grassy, boulder-studded floor and grass-covered, talus-sloped walls, displaying no evidence of recent geomorphologic modification (Figure 7b). Canyon geomorphology could be explained if floodwaters eroded both canyons via knickpoint retreat until Hellisgil incised below the feeder trough elevation, allowing it to pirate flow from the southern cataract and halt its knickpoint retreat, with subsequent flood and/or fluvial activity continuing to drain through Hellisgil and rework channel infill (Figure 7).

Sandá channels

A second network of anastomosing bedrock channels begins ~2.2 km southwest of Kórgil and extends ~5.5 km south to the Sandá river, with a maximum width of ~2.5 km (Figure 8). The Sandá channels are separated by smoothed hills mantled with an unsorted gravel-cobble mélange and occasional erratic boulders.

Each channel contains a similar sequence of features as the western Bláfell network, though on a smaller spatial scale: 1) scoured bedrock outcrops with grooves, flutes, and potholes, with bedrock often fragmented into angular slabs (Figures 8.4 and 8.6); 2) bedrock steps up to ~1 m high (Figure 8.2); and 3) subangular to subrounded, fairly well-sorted boulder clusters with clasts up to 1–2 m diameter, some of which resemble bedrock slabs that support flood-eroded grooves that are not oriented parallel to flow direction (Figure 8.5). The largest, most pronounced erosional landforms occur in the northern end of the channel network and include a bedrock notch and partial amphitheater-shaped cataract (Figure 8.1) and a series of discontinuous bedrock steps ~1–2 m high spread out over ~100 m (Figure 8.3). Striations atop bedrock surfaces at higher elevations and at channel margins indicate that floodwaters did not overtop, or at least lacked the stream power to remove this glacial signature.

Like the western Bláfell channels, this anastomosing network is visible on topographic digital eleva-

Figure 6. Diagram showing hypothesized canyon formation at Kórgil. Lettered arrows correspond to view location and direction of photos a-c. Blue arrows in photos denote flood direction; blue dashed lines outline eroded troughs. Diagram imagery and profile elevation data are from a digital elevation model generated from drone-mounted SfM mapping. The area location is shown in Figure 4. – *Túlkun á myndun farvega við Kórgil. Ljósar örvar (a,b,c) á kortinu sýna staðsetningu og í hvaða átt ljósmyndirnar eru teknar. Bláar örvar sýna stefnu jökulhlaupanna. Bláa punktalínan afmarkar rof farvega. Landlíkanið og hæðarsniðin eru unnin út frá myndum teknum með flygildi. Staðsetning svæðisins er sýnd á 4. mynd.*

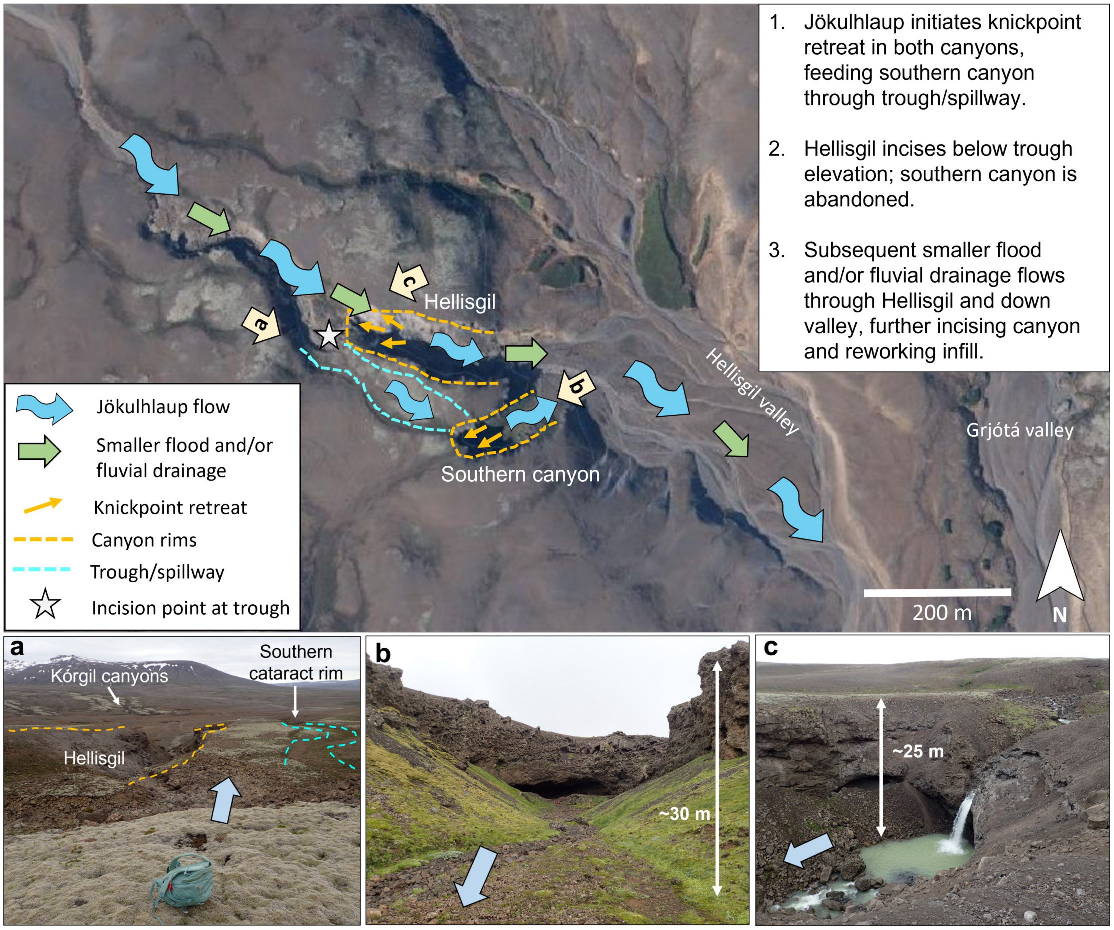

Figure 7. Aerial images showing hypothesized canyon evolution at Hellisgil. Lettered arrows correspond to view location and direction of photos a-c. Blue arrows in photos denote flood direction. Aerial image is from Loftmyndir ehf. The area location is shown in Figure 4. – *Loftmyndir sem sýna túlkun á myndun farvega við Hellisgils. Merktar örvar (a,b,c) sýna staðsetningu og í hvaða átt myndirnar eru teknar. Bláar örvar sýna stefnu jökulhlaupanna. Loftmyndin er frá Loftmyndum ehf. Staðsetning svæðisins er sýnd á 4. mynd.*

tion models, satellite imagery, and aerial photographs. However, unlike the western Bláfell channels, these are shallower, contain smaller-scale landforms, and are not all continuously traceable in field surveys due to vegetation or sediment cover and lack of definitive flood evidence. Their weathered rock surfaces and vegetation and sediment infill also indicate little or no reworking or modification by subsequent floods or fluvial activity. The Sandá channels also cover an area with a lower surface gradient than western Bláfell (Figure 9).

Hvítá river

After its confluence with the Grjótá, the Hvítá river continues south for ∼15 km to Gullfoss waterfall, flowing alternately through a confined basalt channel up to ∼15 m deep and a shallower channel containing gravel bars (Figure 10). The landscape beyond the riverbanks is dominated by glacial features, including striated bedrock outcrops, whaleback bedrock forms, and erratic boulders, with much of the intervening terrain covered by moss, grass, and rofabards (erosional soil pedestals). Four distinct zones of jökulhlaup evi-

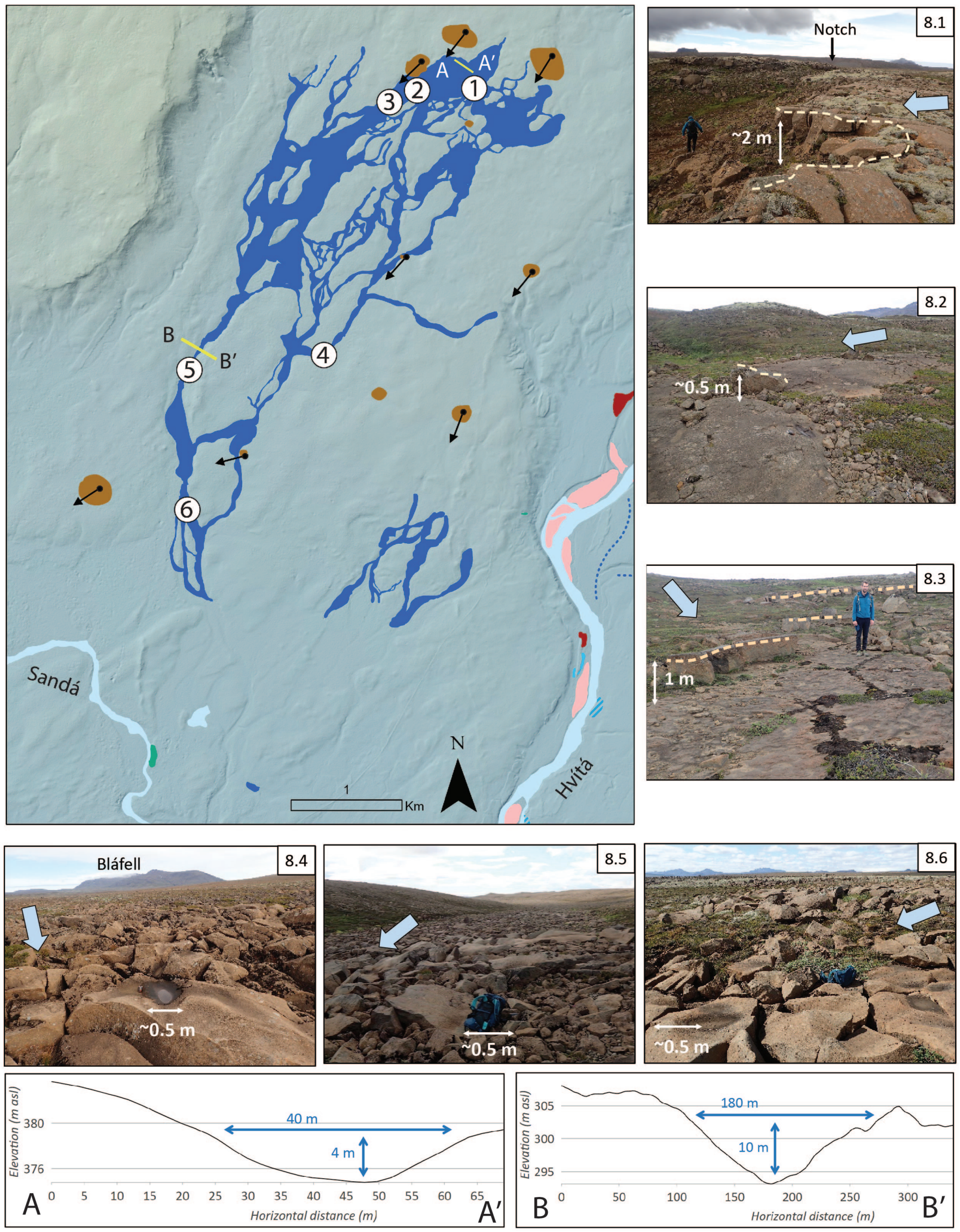

Figure 8. Geomorphologic map of the Sandá channels and examples of flood landforms and cross-sectional profiles. Numbers on map correspond to photo locations. Blue arrows in photos denote flood direction; dotted lines highlight flood erosional landforms. Profile elevation data is from ÍslandsDEM (2021). See Figure 3 for geomorphologic map key. – *Landmótunarkort af svæðinu við Sandá og þversnið rofforma ásamt ljósmyndum af landformum sem mynduðust í jökulhlaupunum. Staðsetning ljósmynda er tölusett. Brotalínur afmarka rofform í farvegum. Hæðargögn þversniða eru frá ÍslandsDEM (2021). Landmótunarskýringar eru á 3. mynd.*

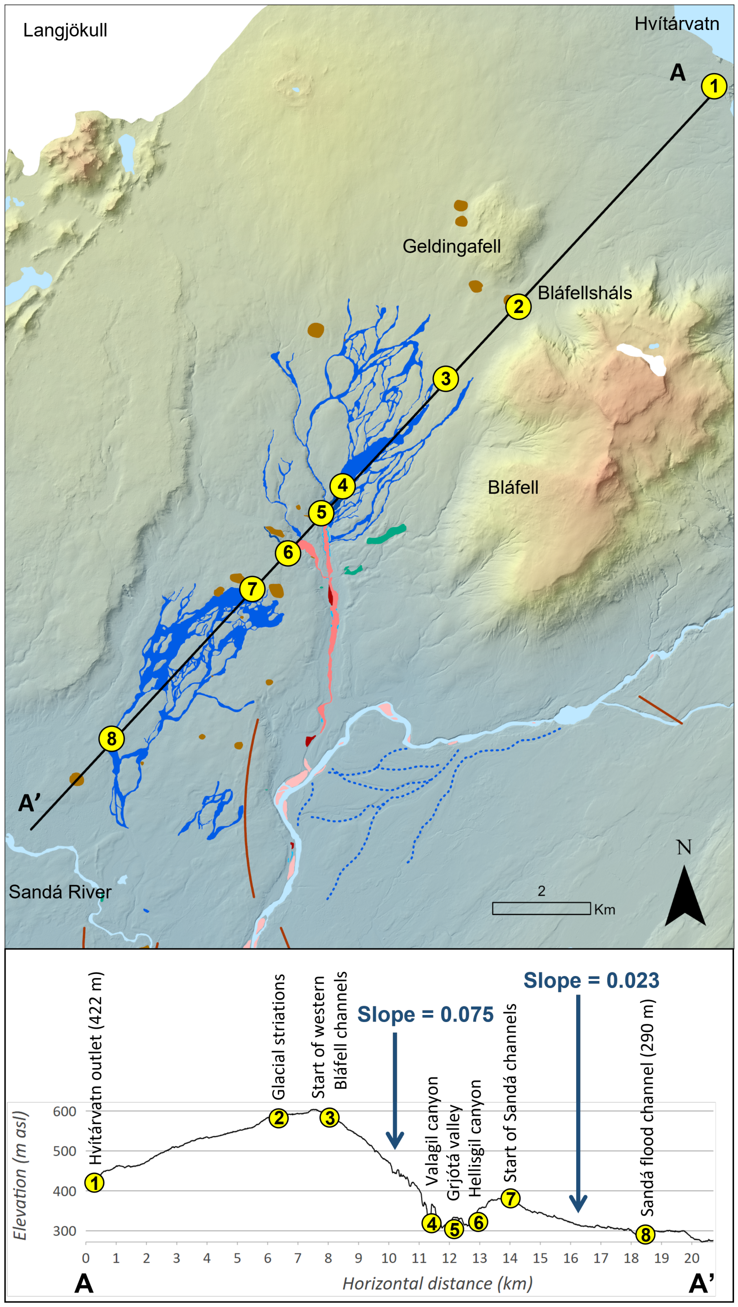

Figure 9. Topographic profile from Hvítárvatn to Sandá showing elevation differences between the western Bláfell and Sandá channel systems. Profile elevation data is from ÍslandsDEM (2021). See Figure 3 for geomorphologic map key. – *Hæðarsnið frá Hvítárvatni til Sandár endurspeglar breytilega landhæð árfarvega við vestanvert Bláfell og Sandá. Sniðið er byggt á ÍslandsDEM hæðarlíkaninu (2021). Sjá skýringar á 3. mynd.*

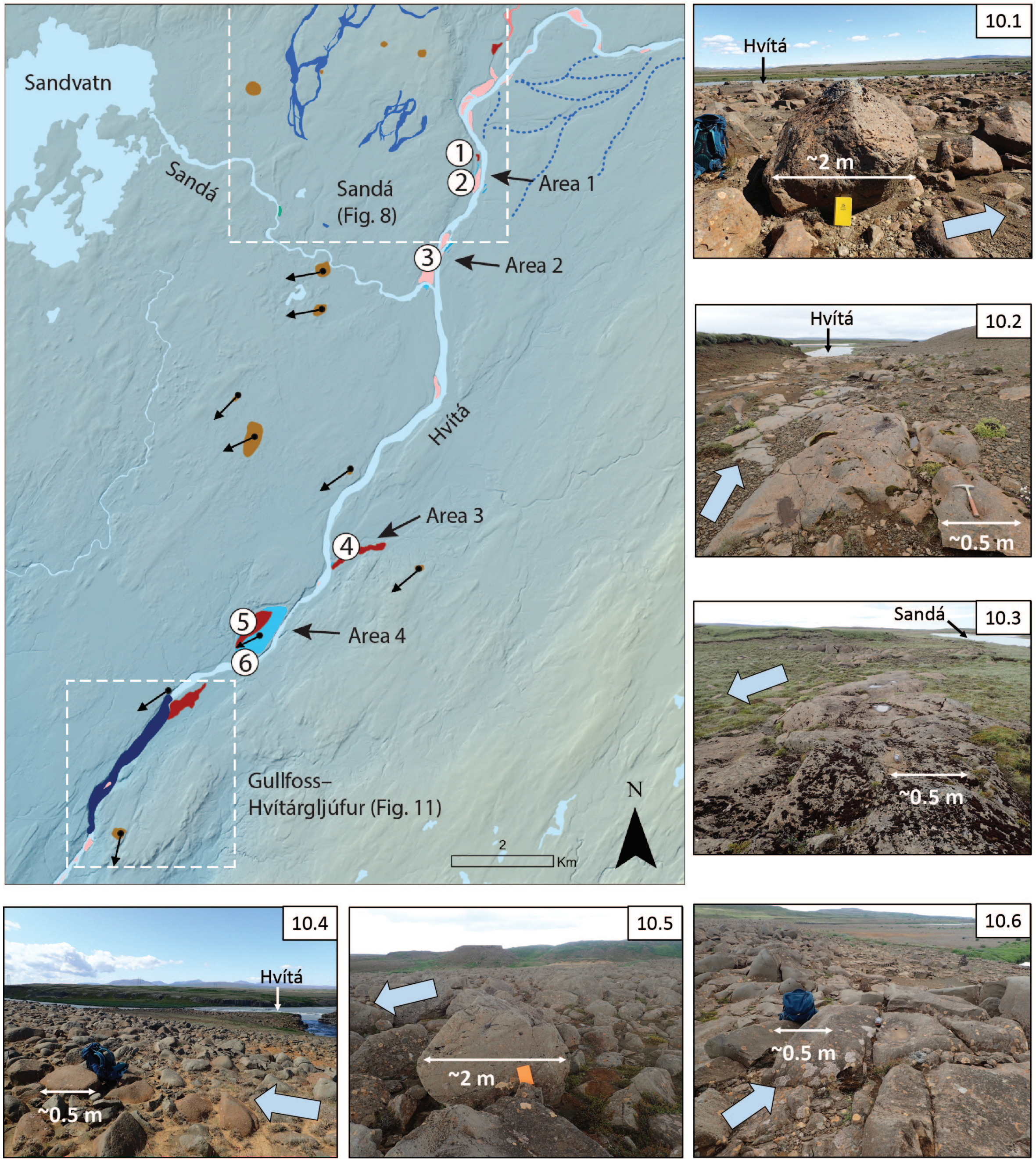

Figure 10. Geomorphologic map of the Hvítá river and examples of flood landforms. Numbers on map correspond to photo locations. Blue arrows in photos denote flood direction. See Figure 3 for geomorphologic map key. – *Landmótunarkort af farvegi Hvítár og ljósmyndir af landformum sem mynduðust í jökulhlaupunum. Staðsetningu ljósmynda er tölusett á kortinu. Bláar örvar sýna stefnu hlaupanna. Sjá skýringar á 3. mynd.*

dence exist amidst this deglacial, vegetated landscape, described here from north to south.

Area 1: The first area contains a ∼200 m long, up to ∼100 m wide tract of scoured bedrock with grooves, flutes, and potholes, with some sections fractured into angular but in situ slabs (Figure 10.2). The largest grooves are ∼1 m long and ∼15 cm deep and occur nearly 60 m from the present riverbank. The outcrop is bisected by a ∼2 m high rofabard containing a white, 26-cm-thick tephra layer at its base that has been dated as Hekla 4, indicating that bedrock scours have been shielded from Hvítá fluvial and seasonal flood activity for at least 4270 years (Meara *et al.*, 2020). About 50 m upstream of this outcrop, a boulder bar covers a ∼120 m long and ∼50 m wide area, with densely concentrated, subangular to subrounded clasts up to 3 m diameter (Figure 10.1). Some boulders retain a hexagonal columnar basalt shape (∼1 m diameter), which closely matches bedrock jointing structures observed immediately upstream.

Area 2: The second area contains discontinuous outcrops of scoured bedrock with grooves and flutes over a ∼100 m x 100 m area (Figure 10.3). It is separated from the modern Hvítá by a rofabard whose basal stratigraphic sequence contains a 22-cm-thick Hekla 4 tephra layer.

Area 3: A third zone of flood evidence occurs on the Hvítá's eastern bank near the confluence with the Búðará tributary stream. This site contains a relatively polished, faintly grooved and fluted bedrock outcrop that is fragmented into angular but in situ slabs. A boulder bar stretches northeast of this outcrop for ∼1 km, consisting of densely-concentrated, subangular to rounded, fairly well-sorted clasts (average 0.5–1 m, maximum 2 m diameter) that outcrop discontinuously from sediment and moss cover (Figure 10.4).

Area 4: The fourth zone contains ∼0.5 km^2 of scoured bedrock with grooves, flutes, and potholes (Figure 10.6), nearly half of which is overlain by a ∼1 km long boulder bar that is oriented parallel to the modern-day Hvítá (Figure 10.5). The largest clasts reach up to 2–3 m diameter and fine downstream to 1.5–2 m. While some clasts are subrounded, others resemble subangular, fragmented bedrock slabs. Boulders are weathered, lichen-covered, and anchored in a mix of sediment, gravel, cobbles, and moss, displaying little evidence of recent modification. The boulder bar is separated from the Hvítá by a series of columnar basalt pedestals up to ∼5 m high with glacially striated top surfaces. Adjacent to the river, a trough-like depression reaches ∼400 m long, ∼30–50 m wide, and up to ∼10 m deep. Though this feature displays no clear jökulhlaup evidence and is lined with grass, three features suggest formation before Hvítá channel incision: it is oriented parallel to the hypothesized flood direction, resembles a flood-eroded trough or spillway, and is ∼15 m above the modern-day river surface.

Gullfoss and Hvítárgljúfur

Roughly 30 km downstream of its outlet at Hvítárvatn, the Hvítá cascades 32 m over the two-tiered Gullfoss waterfall (180 m asl) and funnels for 2.7 km through the Hvítárgljúfur canyon (130 m asl at its southern end) (Figure 11). Glacially striated bedrock occurs on the upper rim of Gullfoss's western bank (Figure 11.1). Its eastern bank forms a terrace that contains an oval-shaped boulder field covering ∼0.17 km^2 and oriented parallel to the modern-day Hvítá (Figure 11.2). Boulders are subangular to subrounded, well-sorted, and mostly in contact but with no clear imbrication. Rocks are weathered, lichened, and exhibit freeze-thaw fracturing, suggesting little recent burial or soil cover, though cobbles, soil, and moss anchor clasts and fill interstices. The largest boulders reach 3.1 m diameter and occur in the upstream-most ∼0.25 km of the bar, decreasing downstream to ∼0.5–1 m diameter before tapering off to a landscape with fragmented, moss-covered bedrock outcrops and no definitive flood or glacial evidence.

Hvítárgljúfur has a box shape, underfit river, cataract (Gullfoss), and strath terraces that are characteristic of analogue gorges eroded by high-magnitude floods in basalt terrain, particularly Jökulsárgljúfur, northeastern Iceland (Baynes *et al.*, 2015a, 2015b), Moses and Grand Coulees, Channeled Scabland, U.S.A. (Baker, 1978, 2009; Larsen and Lamb, 2016; Lehnigk and Lamb, 2022), and Box Canyon, Idaho, U.S.A. (Lamb *et al.*, 2008, 2014; Amidon and Clark, 2015). Hvítárgljúfur's walls are composed of alternat-

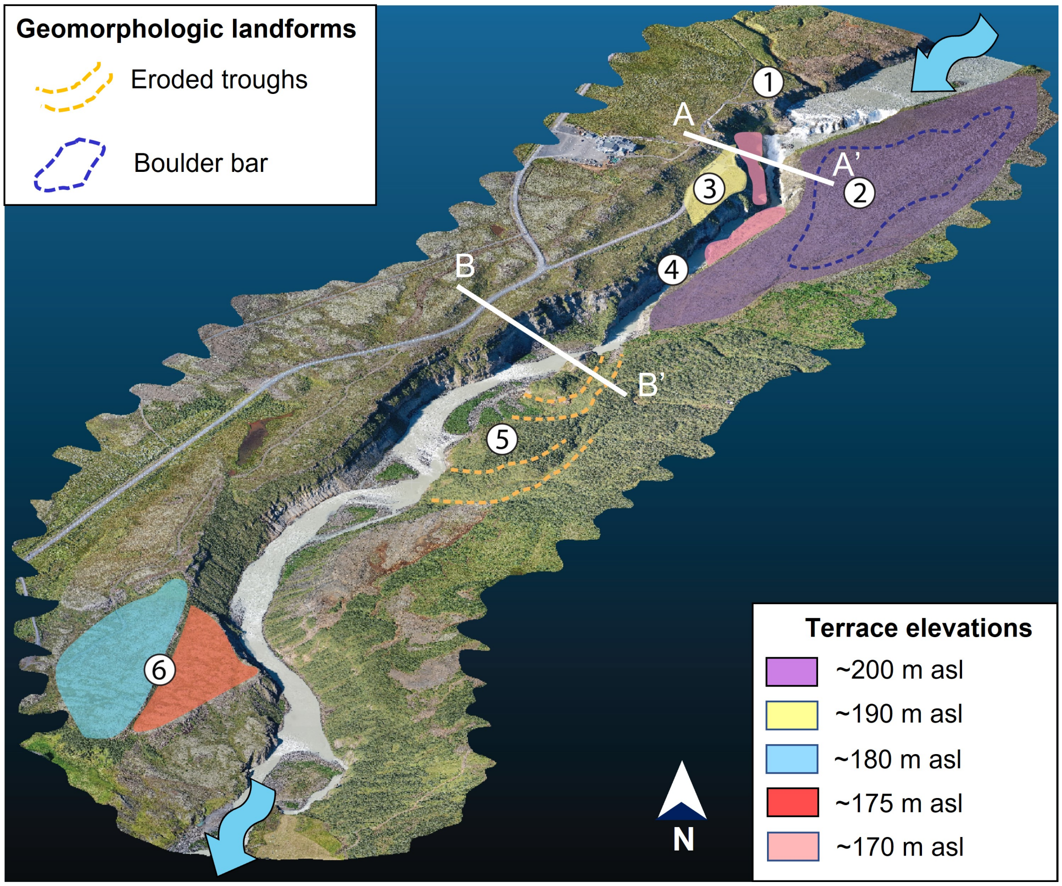

Figure 11. Examples of flood landforms and cross-sectional profiles in Hvítárgljúfur mapped on an oblique image of SfM 3D-mesh. Numbers on map correspond to photo locations. The photographs are presented on the next page. Blue arrows in photos denote flood direction; black arrows indicate features described in the text. Profile elevation data is from a digital elevation model generated from drone-mounted SfM mapping. Horizontal scale is shown on profiles. The area location is shown in Figure 10. – *Þrívíddarlandlíkan af Hvítárgljúfri þar sem helstu landform jökulhlaupanna eru merkt inn ásamt þversniðum. Ljósmyndir á næstu blaðsíðu eru tölusettar á líkaninu. Bláar örvar sýna flæðistefnu; svartar örvar benda á landform sem lýst er í texta. Hæðarþversniðið er unnin út frá landlíkani frá myndum teknum með flygildi. Lengdarkvarði sést á þversniðum. Staðsetning svæðisins er sýnd á 10. mynd.*

ing layers of columnar basalt and lithified sedimentary units (∼8 m and ∼4 m thick on average, respectively), though many basalt columns have a "platy" structure and easily fracture into smaller pieces (Áskelsson, 1946; Tómasson, 1993). Canyons likely formed via knickpoint retreat from columnar basalt toppling and plucking (and possibly cavitation if stream power was high enough) (Benito, 1997; Baker, 2009; Lamb and Dietrich, 2009; Baynes *et al.*, 2015a). Another potential contributing mechanism was erosion of weaker sedimentary units, triggering undercutting and collapse of overlying basalt layers (Áskelsson, 1946; Tómasson, 1993).

The upstream section of the canyon has a box shape that measures ∼100 m wide rim-to-rim and is floored by a set of paired strath terraces with grass-covered surfaces (Figure 11.3) and an inset, ∼30 m wide slot canyon that constrains the modern-

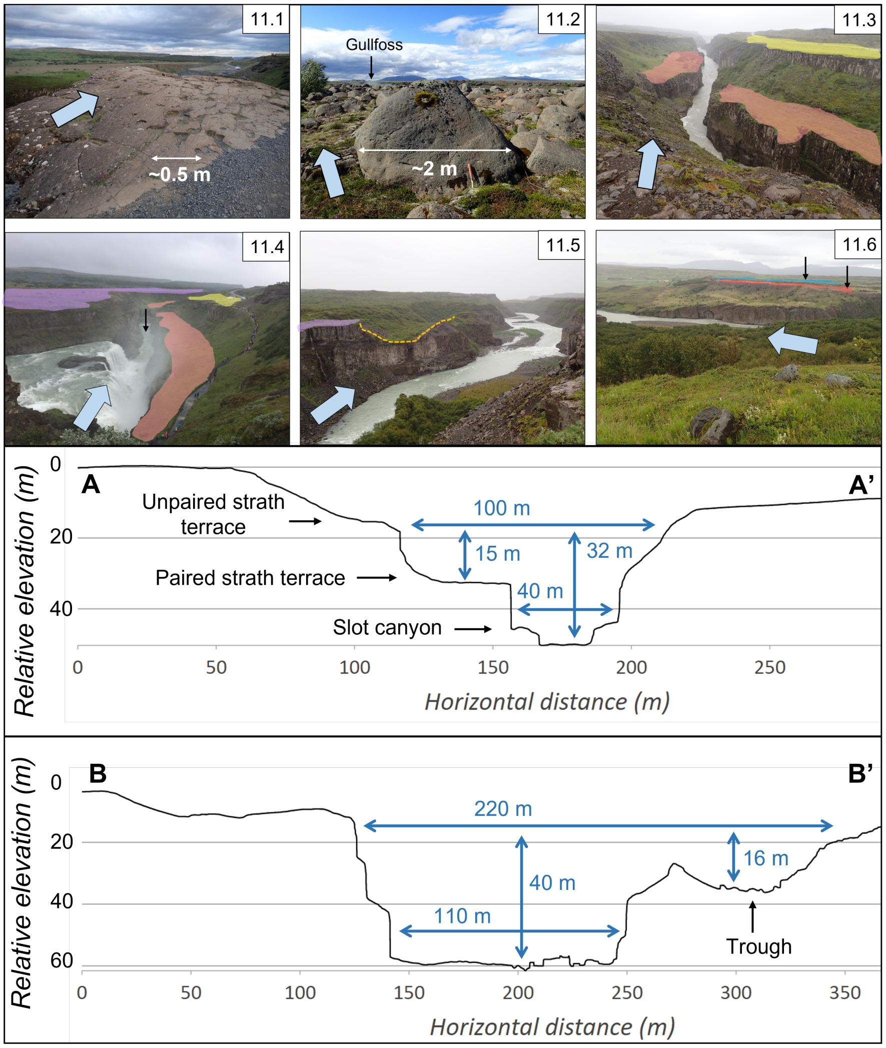

Figure 11. Cont. – *Ljósmyndir og kort með 11. mynd.*

day Hvítá (Figure 11.4). Roughly 1 km downstream of Gullfoss, the gorge expands to an average width of ∼200 m, displaying a box-shaped morphology and reaching a maximum depth of ∼60 m, though a hill forming its eastern wall rises to ∼90 m at its downstream end. This canyon section contains two distinct troughs at different elevations that are separated from the main channel by remnant basalt islands and have sloping hills of vegetated material on their downstream ends (Figure 11.5). The downstream-most western canyon wall contains two potential unpaired strath terraces, which generally follow the top surfaces of columnar basalt layers but are less distinct than the upstream strath set (Figure 11.6). Neither the western nor eastern canyon rim displays distinct jökulhlaup or glacial evidence except for glacially striated outcrops atop a hill near the eastern downstream end (∼125 m above the canyon floor), though most surfaces are vegetated or covered by farmland or infrastructure. Downstream of Hvítárgljúfur, definitive jökulhlaup evidence disappears. Tómasson (1993) hypothesized that the box-shaped canyon sections were eroded by jökulhlaups, with the wider, downstream section eroded by earlier, larger floods, and the narrower, upstream section formed by smaller, subsequent events, before the slot canyon was incised by the post-flood Hvítá river – a sequence that our evidence supports.

Synthesis of geomorphologic evidence

Interpreting jökulhlaup geomorphologic evidence as landform assemblages – groups of features formed under similar hydraulic, lithologic, and geomorphic threshold conditions – yields insight into flood hydrology and drainage dynamics (Marren and Schuh, 2009; Wells *et al.*, 2022). Geomorphologic mapping in the study area reveals three distinct jökulhlaup landform assemblages characteristic of flood impacts in basalt landscapes: 1) scoured bedrock and anastomosing bedrock channels; 2) canyons, cataracts, plunge pools, and strath terraces; and 3) boulder deposits (Figure 12A) (Wells *et al.*, 2022). Interpreting assemblages in their geomorphologic and topographic contexts yields insight into the relative order of landform generation during a single flood (Figure 12B) and the hydraulic conditions and landscape evolution along the drainage route (Figure 12C).

DISCUSSION: GEOMORPHOLOGIC IMPLICATIONS FOR JÖKULHLAUP DRAINAGE ROUTES, LANDSCAPE IMPACT, HYDROLOGY AND CHRONOLOGY

Jökulhlaup drainage routes

Some landforms have clear glacial, jökulhlaup, or fluvial provenance, but many features are too ambiguous to determine process-form relationships. Nonetheless, jökulhlaup landforms and glacial evidence occur in distinct and sometimes unconnected zones in the study area, with no definitive jökulhlaup landforms present in glacial areas, and glacial evidence only existing at higher elevations or channel margins in jökulhlaup zones. While this helps to constrain the flood inundation area, it is not an immutable boundary. Floodwaters may have inundated additional areas but lacked the stream power to leave an erosional trace or the sediment supply to deposit material; post-flood geologic processes certainly modified or removed flood evidence from the modern record; and other jökulhlaup evidence may exist but is buried beneath sediment, soil, or vegetation. Furthermore, not all sections of the study area were field surveyed, so some flood margins are constrained with more certainty than others. Thus, mapped jökulhlaup evidence should be interpreted as a minimum floodwater extent. Synthesizing geomorphologic evidence yields the flood inundation area shown in Figure 13, divided into four unique drainage routes based on evidence spatial distribution and topographic context.

Jökulhlaup inundation area generally corresponds with Tómasson's (1993) mapped drainage routes, with two main differences. First, Tómasson (1993) did not report flood evidence in the Sandá channels or Hellisgil canyons; and second, our preliminary field investigations did not reveal flood evidence south of the Sandá river or west of Hvítárgljúfur, though we did not extensively survey this area (Figure 13).

Jökulhlaup geomorphologic impact

Isolating the geomorphologic impact of the Hvítá floods remains difficult due to interpretive challenges such as landform equifinality, post-flood preservation, and accurate reconstruction of pre-flood topography (Wells *et al.*, 2022). Geomorphologic evidence is interpreted to show a landscape evolution sequence of: 1) ice sheet retreat, leaving a deglacial landscape of moraines, till, outwash sediment, erratic boulders, and eroded bedrock; 2) jökulhlaups (Figure 12); 3) fluvial reworking, rounding, and polishing in some flood-eroded channels; winnowing of boulder deposits (Baker, 1973; O'Connor, 1993; Rathburn, 1993; Herget, 2005); Hvítá channel incision; and sedimentation, soil development, rofabard erosion, and vegetation growth across the region.

Several geomorphologic questions remain unresolved. The first is the discontinuous spatial distribution of jökulhlaup landforms along the modern-day Hvítá river, where definitive flood evidence only appears at four locations between Bláfell and Gullfoss, raising the question: does this distribution reflect absence of evidence or evidence of absence? We hypothesize that jökulhlaup geomorphologic evidence

Landform (number)/ assemblage (color)	Hydraulic context
1 Scoured bedrock	Scouring via abrasion from transported sediments (Whipple et al., 2000; Baker, 2009; Carling, 2009)
2 Anastomosing bedrock channels	Bedrock incision initiates in channels forming an anastomosing pattern (Benito, 1997; Baker, 2009)
3 Cataracts	Knickpoint retreat via plucking excavates bedrock steps, which progressively enlarge to cataracts (Benito, 1997; Carrivick et al., 2004a)
4 Plunge pools	Eroded by force of cascading water at the base of cataracts (Benito, 1997; Lamb et al., 2014; Baynes et al., 2015a)
5 Canyons	Excavation by knickpoint retreat via plucking and/or columnar basalt toppling (Lamb et al., 2014; Baynes et al., 2015a; Larsen and Lamb, 2016)
6 Strath terraces	Incision by subsequent flood events, flood stages, and/or fluvial activity leaves previous bedrock surfaces abandoned (Baynes et al., 2015a; Larsen and Lamb, 2016; Lehnigk and Larsen, 2022)
7 Boulder deposits	Deposited in channels on flood waning stage or in zones of backponding, topographic expansion, or low gradient on rising or waning stage (Baker, 1973; O'Connor, 1993; Rathburn, 1993; Herget, 2005)

A

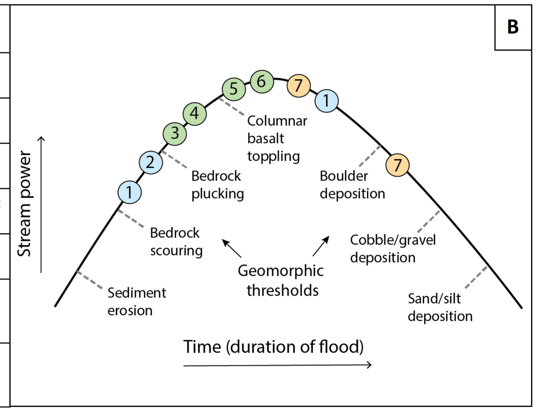

Study area section + landform assemblages	Geomorphologic interpretation
1) Western Bláfell 1 2 3 4 5 7	• Floodwaters scour bedrock and initiate incision in anastomosing channel network • Stream power exceeds threshold for plucking, eroding bedrock steps that scale up to cataracts as stream power increases downslope (slope = 0.075) • Kórgil canyons form via knickpoint retreat from plucking of non-uniformly jointed basalt; stream power is possibly enhanced by hydraulic jump due to elevation drop at valley floor • Plunge pool erosion and bedrock scouring on channel floors continue after channel incision • Boulders (mostly bedrock slabs that were plucked during channel incision, as indicated by pahoehoe textures and columnar basalt structure on some clasts) are deposited in channels during flood waning stage • Subsequent lower-magnitude flood and/or fluvial activity occurs in easternmost channels and continues down Grjótá valley, reworking, rounding, and polishing boulder infill—though flow is not geomorphologically effective enough to modify scoured bedrock highs and boulder bars at channel margins • Hellisgil canyons incise via knickpoint retreat; subsequent smaller flood and/or fluvial activity reworks and polishes channel floors and valley infill
2) Sandá channels 1 2 3 7	• Floodwaters scour bedrock and initiate incision in anastomosing channel network • Bedrock steps and cataracts are eroded within channels via plucking; landform scale decreases downstream as stream power attenuates due to floodwater expansion over unconfined, low-gradient topography (slope = 0.023) • Boulders (mostly bedrock slabs that were plucked during channel incision, as indicated by grooves and columnar basalt structure on some clasts) are deposited in channels during flood waning stage • No subsequent flood or fluvial activity
3) Hvítá River 1 7	• Floodwaters scour bedrock surfaces, but stream power does not attain threshold for plucking due to floodwater expansion and shallowing across wide, unconfined, low-gradient topography (slope = 0.006) • Boulders are deposited where flow competence decreases on flood waning stage or at marginal or backponded zones on rising stage; no clear spatial trend in clast roundness or size, suggesting multiple boulder transport distances and sources (pre-existing glacial moraines, till, and/or erratics, and bedrock slabs that were hydraulically fractured and transported short distances, as indicated by subangular shape and columnar basalt structure that matches upstream lithology) • Post-flood Hvítá River incises channel and reworks or deposits new material to form gravel bars
4) Gullfoss–Hvítárgljúfur 1 3 5 6 7	• Floodwaters excavate Hvítárgljúfur via columnar basalt toppling and plucking (and possibly cavitation, if stream power was high enough), with Gullfoss marking the upstream-most point of knickpoint retreat • Boulder bar is deposited on Gullfoss terrace when floodwaters backpond upstream of topographic constriction during canyon incision • Troughs are eroded within canyon, depositing material on downstream ends • Canyon incision deepens, abandoning previous river and/or flood surfaces at higher elevations to form strath terraces • Subsequent fluvial and/or smaller flood activity reworks or removes material deposited in channel, forming present-day gravel bars; Hvítá River incises slot canyon

C

Figure 12. A) Jökulhlaup landform assemblages formed in the study area. B) Landform generation sequence during a single flood with an idealized, single-peaked hydrograph. C) Spatial distribution and geomorphologic interpretation of landform assemblages along the flood drainage route. – *A) Samsetning landforma mynduðum af jökulhlaupum á rannsóknasvæðinu. B) Röð landforma sem mynduðust í hlaupi með einum flæðitopp. C) Landfræðileg dreifing og túlkun á samsetningu landforma í hlaupfarveginum.*

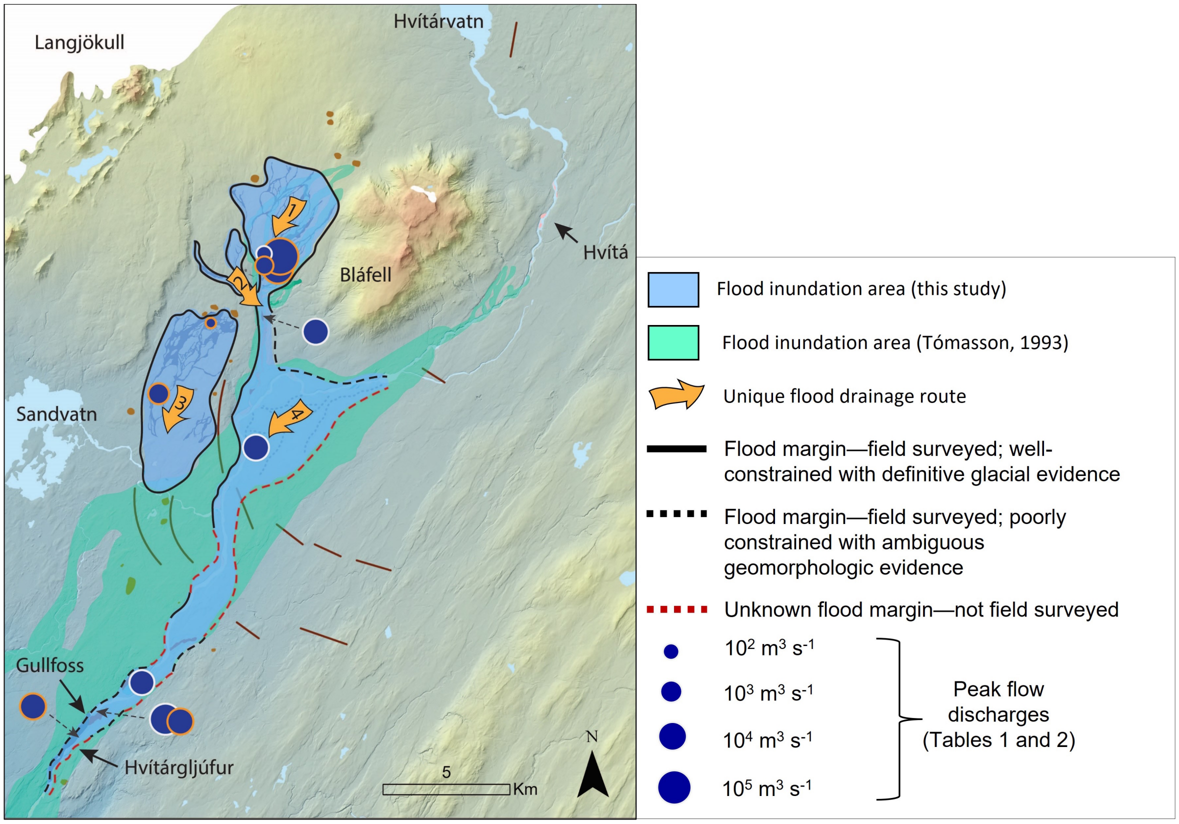

Figure 13. Jökulhlaup inundation area based on geomorphologic evidence mapped in this study compared with Tómasson (1993). Orange arrows show unique flood drainage routes determined from geomorphologic evidence. Outlines indicate certainty of flood margins based on geomorphologic surveys. Dark blue circles show estimated peak flow discharge reconstructed from boulder paleocompetence (white outlines) and Manning's equation (orange outlines) (Tables 1 and 2). See Figure 3 for geomorphologic map key. – *Útlínur farvega jökulhlaupa samkvæmt þessari rannsókn, í samanburði við niðurstöður Hauks Tómassonar (1993). Appelsínugulu örvarnar tákna farvegi sem voru skilgreindir eftir landfræðilegum ummerkjum. Útlínur þekktra (svört heil lína), óljósra (svört punktalína) og áætlaðra (rauð punktalína) farvega eru merktar á kortið. Dökkbláu hringirnir sýna áætlað hámarksrennsli í farveginum, byggt á dreifingu hnullunga og jöfnu Manning's um flæði í opnum farvegi (sjá töflur 1 og 2). Landmótunarfræðilegar skýringar eru á 3. mynd.*

is much more extensive than observed, but landforms are covered by soil or sediment, which is supported by the fact that many features appear from beneath rofabards or vegetation. Alternatively, flood features could exist but are only identifiable in field surveys, which have not yet been completed in every section of this area, a hypothesis that is supported by the fact that landforms such as scoured bedrock outcrops are difficult to detect on available satellite imagery or aerial photographs; and we would not expect stream power to exceed the threshold to erode anything beyond scouring bedrock given this area's unconfined topography and low surface gradient (Figure 12) (Tómasson, 1993). Another possible explanation is modification by post-flood geologic processes, particularly the modern-day Hvítá, which appears to have incised the flood landscape to leave seemingly continuous scoured bedrock outcrops and boulder deposits on either side of its banks.

Another remaining geomorphologic question is where floodwaters deposited material. We would expect to see extensive flood deposits south of the Sandá channels and Hvítárgljúfur, where floodwaters would have entered a zone of relative topographic expansion, decreasing competence and depositing material eroded from the upstream channels. However, no obvious depositional features appear in remote sensing imagery or initial field surveys. This apparent lack of evidence could have three possible explanations: 1) flood evidence exists but is obscured by overlying soil, vegetation, or sediment cover; 2) flood evidence has been reworked by subsequent fluvial activity, smaller jökulhlaups, and/or flood waning stages and swept farther downstream; and 3) floods drained across these landscapes but lacked the stream power or sediment supply to leave an erosional or depositional trace, respectively (Tómasson, 1993).

Jökulhlaup deposits may exist but only be detectable by extensive field surveys, which we have yet to do in these areas. Tómasson (1993; 2002) reported gravel, cobble, and boulder deltas along a zone ~3 km south of Hvítárgljúfur; and turbidites in lacustrine sediment cores in Hestvatn, a lake ~40 km south of Hvítárgljúfur, have been attributed to the Hvítá jökulhlaups due to their early Holocene deposition (~10.6–10.2 ka), non-volcanogenic origin, and location along the presumed drainage route (Hannesdóttir, 2006; Geirsdóttir *et al.*, 2009; Hannesdóttir *et al.*, 2006). Moreover, the Þjórsárhraun lava flow ~8600 ka would have buried any flood deposits south of Hestvatn (Figure 1) (Tómasson, 1993; Hjartarson, 1988; Halldorsson *et al.*, 2008), and sea level may have been higher at the time of the floods, resulting in submarine deposits. Finally, Iceland's dynamic early Holocene glacial isostatic adjustment may have affected flood incision and routing on a regional scale (Tómasson, 1993; Ingólfsson *et al.*, 2010; Eason *et al.*, 2015; Stucky de Quay *et al.*, 2019; Pico *et al.*, 2022).

Another unresolved challenge is isolating the geomorphologic impact of the Hvítá jökulhlaups from other geologic processes. This is particularly true for Hvítárgljúfur, where the question remains; how much of the canyon was formed by high-magnitude floods versus post-flood fluvial incision or other geologic processes (such as faulting or groundwater seepage erosion (Lamb *et al.*, 2008))? These relative contributions are impossible to quantify without knowing pre-flood topography, number of flood events, and Holocene Hvítá bedrock incision rates, among other parameters. If fluvial erosion alone had been responsible for canyon formation – assuming that no canyon existed at the time of deglaciation – the Gullfoss knickpoint would have had to retreat horizontally at an average annual rate of ~0.27 m. However, georeferencing aerial photos (Landmælingar Íslands) from 1960 to present reveals less than the required ~13 m of retreat during this interval at the Gullfoss knickpoint location (though precise measurements are difficult due to water stage flux, flow turbulence, and a lack of precisely defined reference points at the cataract) (Tómasson, 1993; Baynes *et al.*, 2015b). Hvítárgljúfur is the largest observed jökulhlaup landform, yet it occurs at the downstream-most end of the study area where flow stream power and volume would have likely attenuated after draining for ~15 km across a relatively low-gradient, unconfined plain. Why did floodwaters channelize at this particular location? We hypothesize that a structural weakness or a fluvial channel existed at the time of the Hvítá jökulhlaups, which floodwaters exploited. Its relatively straight channel hints at a tectonic control such as a fault, supporting this hypothesis (Tómasson, 1993; Thordarson and Höskuldsson, 2002).

A similar question applies for unraveling the relative role of floods versus fluvial activity in the Grjótá channel and valley, where reworked boulder–cobble infill may indicate multiple flood events. Though observed seasonal flow has only occupied the lowest, central-most channel section, fluvial activity may have been greater in the past. The fact that the Grjótá channel is labeled as the "Grjótá river" on maps, coupled with its thick, polished, channel-wide boulder infill, may suggest that a perennial river flowed here during historic times. Moreover, snowpack and seasonal melt may have been greater during cooler Holocene periods such as the Neoglacial and Little Ice Age (Larsen *et al.*, 2012; Garcia-Castellanos and O'Connor, 2018).

Jökulhlaup hydrology

Another key challenge in determining jökulhlaup geomorphologic impact is linking individual landforms with the hydraulic conditions and flood events that formed them. We calculated paleocompetence of the largest flood-deposited boulders at five sites to provide a first order approximation of the minimum flow

Table 1. Peak flow discharge based on paleocompetence calculations for the largest boulder at five sites (for locations, see references to figures in the table). – *Niðurstöður útreikninga straumhraða út frá hámarksstærð hnullunga á fimm stöðum í farvegum jökulhlaupanna (sjá tilvísanir í myndir í töflunni).*

Site	GPS coordinates	Boulder long axis (m)	Boulder middle axis (m)	Boulder short axis (m)	Maximum channel width (m)	Channel bed slope	Discharge ($m^3 s^{-1}$) (rounded to nearest hundred)
Grjótá channel– boulder infill (Figure 4.6)	N 64° 28' 57.8" W 19° 58' 38.1"	3.2	2.15	1.8	25	0.04	1600
Grjótá valley– boulder bar (Figure 4.8)	N 64° 27' 56.4" W 19° 58' 33.3"	3.9	2.7	2.3	570	0.005	69,600
Hvítá River, Area 1– boulder bar (Figure 10.1)	N 64° 25' 15.4" W 19° 59' 34.6"	2.9	1.9	1.25	525	0.015	31,000
Hvítá River, Area 4– boulder bar (Figure 10.5)	N 64° 20' 26.8" W 20° 04' 54.1"	3.3	2.3	1.9	675	0.01	58,400
Eastern Gullfoss– boulder bar (Figure 11.2)	N 64° 19' 40.8" W 20° 06' 30.0"	2.9	1.9	1.7	1155	0.001	128,400

Table 2. Peak flow discharge based on Manning's equation at channel cross sections at seven sites (for locations, see references to figures in the table). – *Niðurstöður útreikninga á hámarksstraumhraða fyrir sjö þversnið í farvegum jökulhlaupanna. Útreikningar eru byggðir á jöfnu Manning's (sjá tilvísanir í myndir af staðsetningu þversniða).*

Site	GPS coordinates (in middle of transect)	Maximum channel width (m)	Maximum channel depth (m)	Channel cross-sectional area (m^2)	Channel bed slope	Wetted perimeter (m)	Hydraulic radius (m)	Velocity ($m s^{-1}$)	Discharge ($m^3 s^{-1}$) (rounded to nearest hundred)
Equation/ abbreviation		W	D	A=W*D	S	P	R=A/P	$V=(n^{-1})*(R^{2/3})*(S^{1/2})$	Q=A*v
Grjótá channel, A–A' (Figure 6)	N 64° 28' 57" W 19° 58' 38"	25	9	180	0.04	37.5	4.8	14.23	2600
Valagil, B–B' (Figure 6)	N 64° 29' 06" W 19° 58' 20"	96	54	4824	0.09357	181.2	26.62	68.18	328,900
Kór, C–C' (Figure 6)	N 64° 29' 00" W 19° 58' 17"	103	44	4150	0.09357	169.2	24.53	64.56	267,900
Sandá channel, A–A' (Figure 8)	N 64° 28' 02" W 20° 00' 54"	40	4	100	0.023	41	2.44	6.87	700
Sandá channel, B–B' (Figure 8)	N 64° 26' 39" W 20° 03' 55"	180	10	1000	0.023	181.2	5.52	11.84	11,800
Hvítárgljúfur, A–A' (Figure 11)	N 64° 19' 32" W 20° 07' 23"	100	32	2030	0.002	154	13.18	6.24	12,700
Hvítárgljúfur, B–B' (Figure 11)	N 64° 19' 05" W 20° 08' 14"	220	40	5800	0.002	292.3	19.84	8.19	47,500

discharge required to transport clasts (Table 1). Since suitable boulders were not present along each hypothesized drainage route – and to compare methods – we also used Manning's equation to estimate flow peak discharge at seven channel cross sections (Table 2). We did not calculate discharge along the Hellisgil route due to modified appearance of boulder deposits and lower topographic resolution given a lack of SfM drone-mapping and canyon shadow effects in the ÍslandsDEM (2021) model.

Preliminary results yielded peak flow discharges spanning three orders of magnitude from 10^2 to 10^5 m^3s^{-1} (Figure 13). This corroborates peak discharges calculated by Tómasson (1993) from flood channel cross sections, though results do not necessarily correspond to the same drainage routes. The Kórgil canyons yielded the largest peak discharges of $\sim$200–300,000 m^3s^{-1}, an order of magnitude greater than Tómasson (1993) calculated along this route – though discharges of 10^5 m^3s^{-1} were also measured in Hvítárgljúfur, in line with Tómasson's results. Moreover, flood magnitude did not always correlate with geomorphologic context along a single drainage route. Peak discharge in the Sandá channels was two orders of magnitude higher in a shallow downstream channel than an upstream erosional notch, where geomorphologic evidence and closer proximity to the flood source would indicate greater stream power. Furthermore, calculated discharges sometimes differed at the same site for different paleohydraulic methods; for example, peak flow discharge from paleocompetence at the eastern Gullfoss boulder bar was on the order of magnitude of 10^5 m^3s^{-1}, but only 10^4 m^3s^{-1} based on Manning's equation at a cross section in the same location.

These paleohydraulic reconstructions are subject to numerous potential sources of analytical error and uncertainty and should thus be interpreted as first order approximations and reported as orders of magnitude rather than precise values. Both paleohydraulic methods use modern-day topography, which does not accurately represent channel morphology at the time of the Hvítá floods due to observed post-flood infill (boulder deposits and talus slopes) and erosion (fluvial incision, particularly by the Hvítá river), which can underestimate and overestimate peak discharge, respectively. Moreover, cross sections may be inaccurate where they intersect the modern-day Hvítá river since underwater channel morphology and depth are unknown, and water surfaces return inaccurate elevation data. Due to the lack of paleostage indicators of floodwater depth, our calculations also assume "brimfull" channels, which may significantly overestimate peak discharge since channels may have formed during multiple flood events, progressive downcutting during a single flood, and/or post-flood fluvial incision (Larsen and Lamb, 2016; Lehnigk *et al.*, 2022). Some cross sections also have poorly defined channel margins due to a lack of paleostage indicators or topographic constraints, particularly at measured paleocompetence sites along the Hvítá river. Paleohydraulic calculations may also underestimate peak flow if floodwaters drained along multiple paths concurrently, as indicated by the anastomosing pattern in the western Bláfell and Sandá channels. Finally, paleocompetence may underestimate peak flood discharge due to limited supply of larger clasts along the drainage route or boulder deposition on flood waning stage or in zones of backponding or reduced flow velocity (O'Connor, 1993; Rathburn, 1993; Herget, 2005; Stokes *et al.*, 2012).

Despite these analytical uncertainties, paleohydraulic results can be interpreted alongside geomorphologic evidence to help reconstruct jökulhlaup drainage dynamics. Peak discharges are greatest at Kórgil and Hvítárgljúfur, in line with the largest-scale flood erosional landforms, and decrease by an order of magnitude in the area between the two canyon systems, which is logical given the relative topographic expansion and low surface gradient and is also reflected in the lower-intensity erosional landforms along this reach. Peak discharges in the Sandá channels are smaller than those along the western Bláfell and Hvítá river routes, corroborating field evidence of floods with lower stream power and supporting the hypothesis that separate floods formed the Sandá network. Finally, discharges along the western Bláfell route match orders of flow magnitude along the Hvítá river, supporting geomorphologic evidence that they continued to drain along this path.

Jökulhlaup chronology

Spatially and temporally linking different lines of geomorphologic evidence – in other words, determining which floods formed which landforms – is crucial for reconstructing flood magnitude, drainage sequence, and geomorphologic impact, yet it remains a significant challenge that we cannot resolve without absolute dating. Nonetheless, geomorphologic evidence must precede geochronological data to help generate hypotheses and design sample collection strategies.

There is no clear geomorphologic evidence for multiple flood events along each hypothesized drainage route, suggesting five possibilities: 1) only one flood drained along each route; 2) multiple floods occurred, but the most recent flood was the largest and most geomorphologically effective, erasing evidence of previous, lower-magnitude events; 3) smaller, subsequent floods occurred but lacked the stream power and/or sediment supply to leave a distinct geomorphologic signature; 4) multiple floods occurred, but their individual geomorphological impacts are not distinguishable due to feature equifinality or preservation; or 5) subsequent high-magnitude floods did drain along these routes but incised channels further, leaving sides unmodified and abandoned while lowering and reworking material on channel floors (Larsen and Lamb, 2016; Lehnigk and Larsen, 2022).

Despite its hypothesized conveyance of three separate drainage routes, the present-day Hvítá course between the Grjótá confluence and Gullfoss also does not display definitive evidence of multiple flood events. However, jökulhlaup zones along this reach occur at different spatial scales and elevations above the modern river channel, potentially indicating formation by different floods. Areas 1 and 2 are situated at the modern-day Hvítá bank elevation, while Areas 3 and 4 are perched $\sim$10–15 m above the current river level and cover much larger areas, possibly suggesting that the latter two sites were formed by older and/or larger floods. However, we hypothesize that Hvítá incision occurred post-flood since floodwaters would likely have expanded a pre-existing channel to a more box-shaped morphology as seen at Hvítárgljúfur given the area's similar columnar basalt lithology. Moreover, jökulhlaup geomorphologic evidence may be more extensive at Areas 1 and 2 but is presently buried by soil and vegetation. Thus, evidence is not conclusive enough at present to determine whether geomorphologic differences between sites result from separate flood events or lithologic, topographic, and/or sediment supply variations along the drainage route.

Hvítárgljúfur may also preserve clues to relative jökulhlaup chronology. Strath terraces may indicate post-flood surfaces that were abandoned after further flood and/or fluvial incision; and the two troughs in the downstream canyon section occur at different elevations, possibly indicating erosion during different flood events. However, these features could also have formed during different stages of the same flood as the canyon progressively deepened and left previous erosional marks abandoned at higher elevations (Tómasson, 1993; Baynes *et al.*, 2015a; Lehnigk and Larsen, 2022).

To reconstruct flood sequence and absolute chronology, cosmogenic nuclide exposure dating should be conducted along each of the four mapped flood routes, as well as at different elevations and spatial extents along the Hvítá river to identify separate floods that may have drained along the same path. Numerous flood-scoured bedrock surfaces, flood-deposited boulders, and canyon, cataract, and strath terrace levels offer promising sampling candidates to reconstruct absolute flood chronology (Figures 4, 8, 10, and 11). However, it is possible that temporal resolution will not be high enough to distinguish between events that occurred on a decadal or centennial time scale given error ranges from other studies using this technique in Iceland (Andrés *et al.*, 2019).

IMPLICATIONS FOR ICELANDIC ICE SHEET DEGLACIATION

Synthesizing flood drainage routes, geomorphologic impact, hydrology, and relative chronology introduces four hypothesized scenarios for IIS deglaciation and Glacial Lake Kjölur evolution (Figure 14). However, testing these scenarios requires additional ongoing reconstructive methods such as geochronology, ice sheet modeling, and glacial lake mapping.

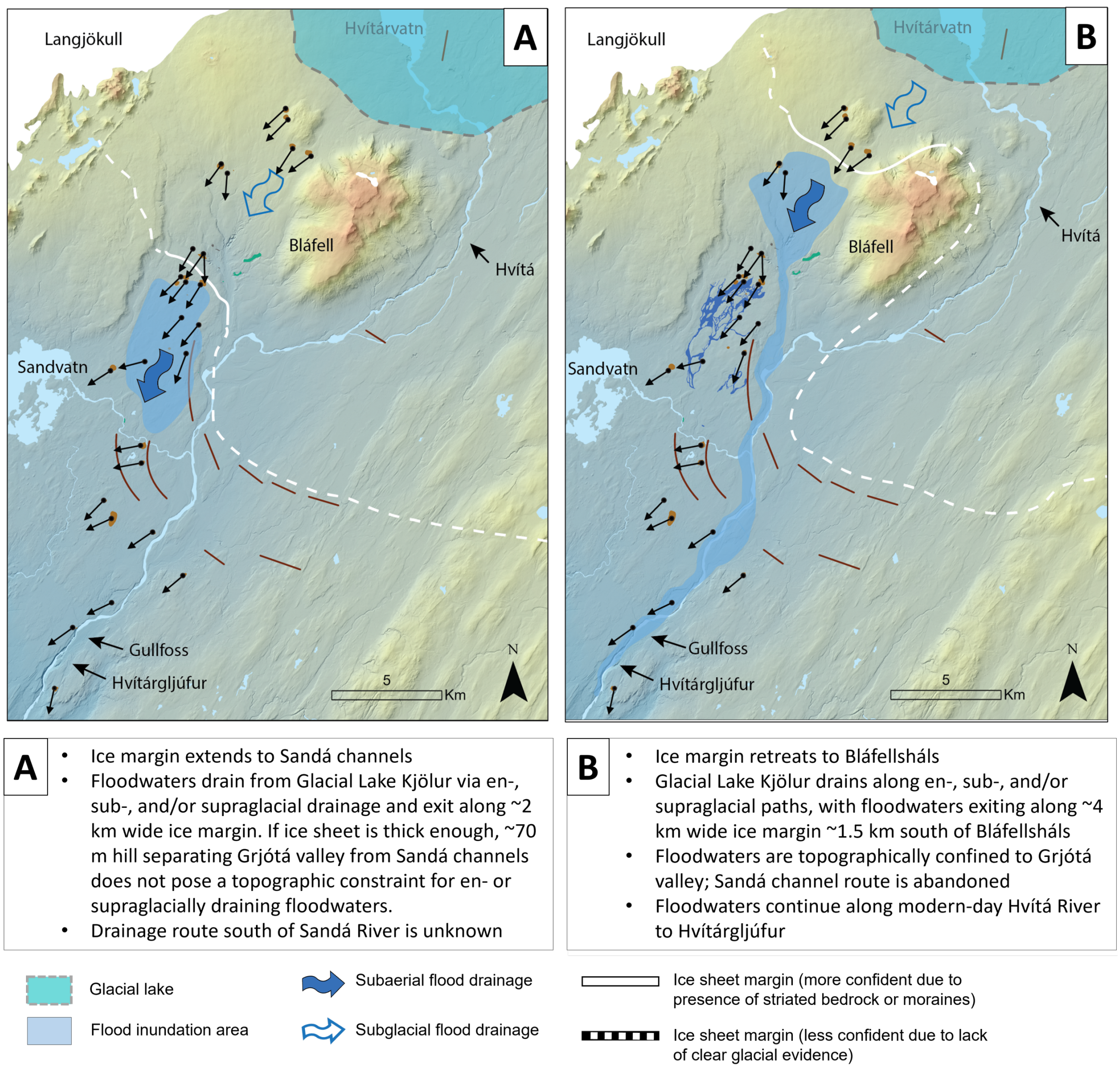

Figure 14. Potential scenarios of ice margin position, glacial lake location, and jökulhlaup drainage routes down the Hvítá channels progressing through time from panel A (oldest) to panel D (youngest) on the next page. Figure 3 shows geomorphologic map key. – *Hugsanlegar sviðsmyndir um stöðu jökuljaðra, útbreiðslu jökullóna og flóðafarvega fjögurra jökulhlaupa niður farveg Hvítár. Sviðsmynd A er fyrir elsta flóðið og D það yngsta, sjá næstu blaðsíðu. Landmótunarskýringar eru á 3. mynd.*

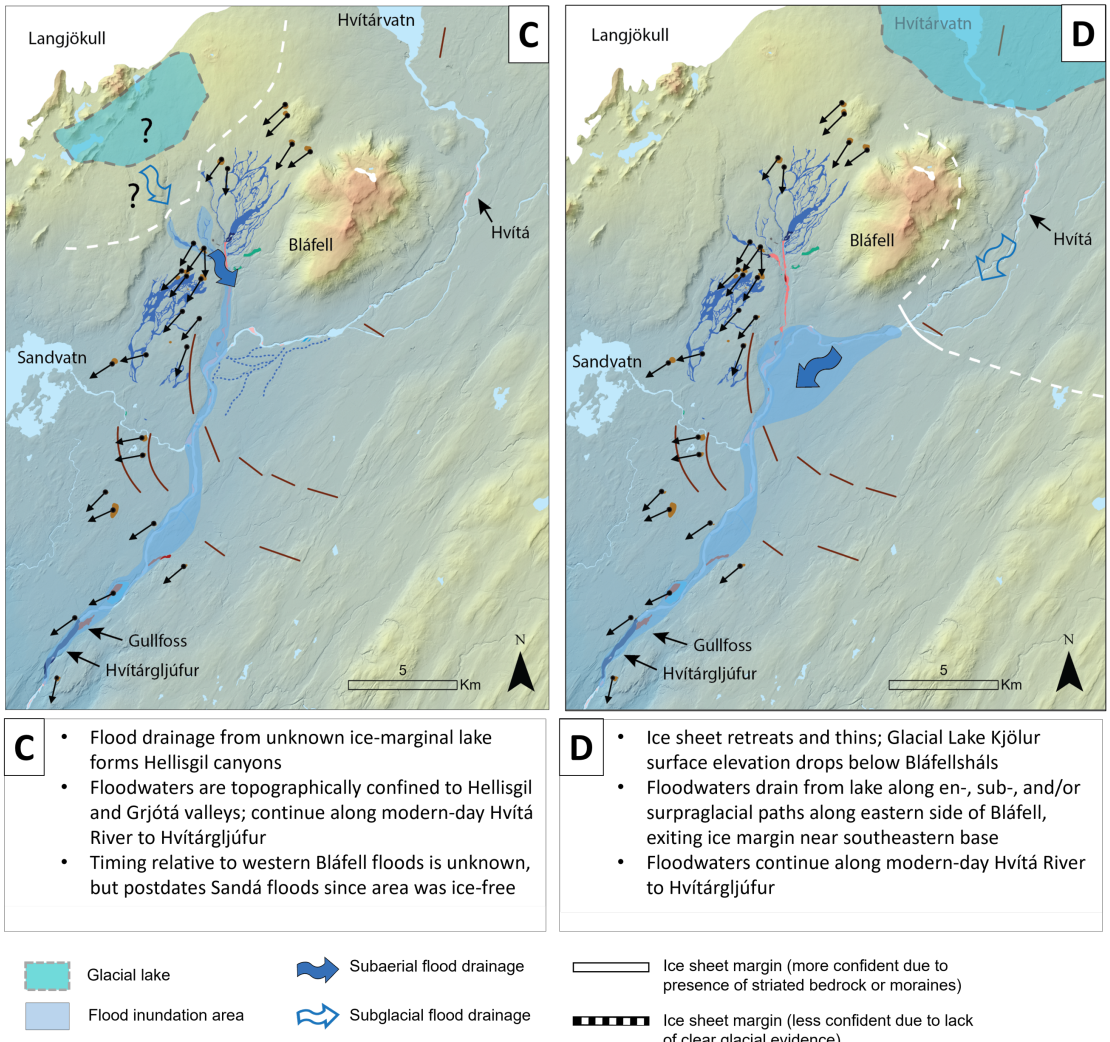

Figure 14. Cont. – Framhald.

Tómasson (1993) interpreted paleoshoreline elevations to conclude that multiple floods drained from Glacial Lake Kjölur, with at least four draining to the north, four subsequently over Bláfellsháls, and seven finally around the eastern side of Bláfell. While our observed geomorphologic evidence corroborates the locations of the latter two drainage routes, it does not indicate multiple jökulhlaup events. This could imply that shorelines do not correspond to unique drainage events but were instead formed by a series of smaller lakes rather than a single, continuous Glacial Lake Kjölur; or that the lake drained along additional routes than those mapped in the study area. However, these scenarios are unlikely given the estimated flood magnitude (and thus lake volume), regional topography, and lack of jökulhlaup evidence observed elsewhere.

Alternatively, the ice sheet could have retreated from the catchment too quickly for the lake to refill and/or the glacier thinned too rapidly to re-impound meltwater (Evans and Clague, 1994; Tweed and Russell, 1999; Benn and Evans, 2010). The IIS had a relatively low surface gradient due to underlying topography. Thus, if atmospheric temperatures increased and equilibrium line altitude (ELA) decreased rapidly (perhaps exacerbated by rapid glacial isostatic uplift), the glacier could have thinned very quickly and failed to reach the required ELA to reform during cooler periods, leading to rapid breakup with little readvance (Patton *et al.*, 2017). Lake growth can also trigger a positive feedback cycle of ice loss, with meltwater destabilizing glacier termini by increasing melting and calving rates (Benn and Evans, 2010; Carrivick and Tweed, 2013; Carrivick *et al.*, 2020; Sutherland *et al.*, 2020). Rapid early Holocene IIS retreat has been recorded by cosmogenic nuclide dates on glacial surfaces in northern Iceland (Andrés *et al.*, 2019). It could further be supported by the relative lack of moraines across the study area and the dearth of lacustrine sediments in the Kjölur basin; however, this could also be due to the fact that the region was near the ice divide, leaving little terrain for glaciers to erode and source sediment (Kaldal and Víkingsson, 1990; Patton *et al.*, 2017).

A second hypothesis for a single flood along each route is that jökulhlaups were volcanogenically sourced, with a subglacial eruption producing a rapid meltwater influx that triggered ice dam failure or flotation. Leggjabrjótur is the only documented lava flow from a subglacial eruption in the Kjölur basin during deglaciation, estimated as occurring during the Younger Dryas when the area was partly glaciated, and possibly contributing meltwater to Glacial Lake Kjölur (Kjartansson, 1964; Tómasson, 1993; Sinton *et al.*, 2005; Eason *et al.*, 2015). Alternatively, a different subglacial eruption could have occurred that has not yet been reported, which is a possibility given increased magma production and eruptive activity from decompression melting in response to glacier unloading during the early Holocene (Maclennan *et al.*, 2002; Sinton *et al.*, 2005; Licciardi *et al.*, 2007; Eason *et al.*, 2015).

Another hypothesis for the apparent lack of multiple floods along each route is that evidence is not preserved in the geomorphologic record. Subsequent floods (or other post-flood processes) could have removed or modified landforms from previous events – for example, by reworking channel infill, further incising channels, or depositing material atop flood-modified surfaces (Wells *et al.*, 2022). Ice-marginal lakes typically drain repeatedly in a process known as the "jökulhlaup cycle," where lake level crosses a hydrostatic threshold to trigger ice dam flotation or failure, and glacial tunnels close when overlying ice pressure exceeds waning hydraulic pressure, allowing the lake to refill (Evans and Clague, 1994; Tweed and Russell, 1999). Ice-marginal lakes repeatedly drained through this process during the Pleistocene–Holocene transition in North America, Eurasia, and Patagonia (Baker, 2013; O'Connor *et al.*, 2020; Benito *et al.*, 2021), as well as throughout recorded history in Iceland (Thorarinsson, 1939; Roberts *et al.*, 2005), Greenland (Russell *et al.*, 2011), Patagonia (Jacquet *et al.*, 2017), and Alaska (Anderson *et al.*, 2003). Moreover, one of the most robust indicators of multiple events is stacked layers of deposited sediments, which have not yet been reported in the Hvítá region (Carling, 2013; van der Bilt *et al.*, 2021). Thus, the lack of evidence for multiple floods in the current geomorphologic record does not reject this "jökulhlaup cycle" hypothesis.

CONCLUSIONS

New mapping of the geomorphology of the Hvítá region that combines field surveys, remote sensing, and a new interpretive framework (Wells *et al.*, 2022) reveals more extensive jökulhlaup evidence and a more complex pattern of drainage dynamics and landscape impacts than previously reported (Tómasson, 1993). Geomorphologic results indicate that floods drained along four distinct routes, three of which merged together along the present-day Hvítá river; and first order approximations of peak flow discharges range from 10^2 to 10^5 $m^3 s^{-1}$. There is no definitive evidence along the individual routes for multiple separate flood events, which is incompatible with the presence of numerous paleoshorelines in the former Glacial Lake Kjölur basin (Kjartansson, 1964; Tómasson, 1993), as well as ice-dammed lake drainage analogues in Iceland and worldwide. This implies that if multiple floods drained along each separate route, in each case the last flood was able to override the traces of previous events or left no evidence discernible today within the landscape record. Future geochronological analyses can help resolve flood drainage sequence and timing.

Geomorphologic and paleohydraulic results introduce different, testable scenarios of ice margin position, glacial lake evolution, and flood drainage sequence that help us to better understand the final decay of the last IIS. Nonetheless, numerous interpretive challenges and knowledge gaps remain, including determining pre-flood topography; mapping landscape sections obscured by Holocene vegetation and soil cover; linking jökulhlaup landforms to the specific flood event that formed them; establishing meltwater source; distinguishing subglacial versus subaerial flood drainage routes; and reconstructing an absolute flood chronology. Geomorphologic results also demonstrate the importance of mapping with a multimethod approach combining field surveys and remote sensing, accurately interpreting geomorphologic evidence, and accepting limitations of the geomorphic record (Wells *et al.*, 2022).

The Hvítá jökulhlaups illustrate the importance of high magnitude, low frequency meltwater outpourings in shaping landscapes of deglaciation in Iceland during IIS breakup and, by implication, previous glaciations. The current decay of Icelandic ice caps is creating ever larger ice-marginal meltwater lakes (Aðalgeirsdóttir *et al.*, 2011, 2020; Guðmundsson *et al.*, 2019; Hannesdóttir *et al.*, 2020), and although changes in ice masses and lake volumes are orders of magnitude smaller than during early Holocene deglaciation, reconstructing past ice sensitivity and proglacial hydrologic response may yield insight into contemporary and future change in Iceland. This study of the Hvítá floods also increases the very limited body of existing work on the impacts of Icelandic jökulhlaups on bedrock terrain and crucially advances our understanding of proglacial lake outbursts rather than the effects of subglacial eruptions. This helps us to identify additional flood landscapes in Iceland and adds to the global compendium of flood geomorphology in basalt settings (Baynes *et al.*, 2015a).

Finally, the Hvítá jökulhlaups serve as an excellent analogue for similar events elsewhere. Ice-dammed lakes at ice sheet margins drained during the Pleistocene-Holocene transition across North America, Scandinavia, Eurasia, and Patagonia (Komatsu *et al.*, 2016; Regnéll *et al.*, 2019; Benito and Thorndycraft, 2020; Fisher, 2020; O'Connor *et al.*, 2020); and contemporary floods from ice-marginal lakes occur at the Greenland Ice Sheet (Grinsted *et al.*, 2017), Patagonian Ice Field (Dussaillant *et al.*, 2010), and Alaska (Rick *et al.*, 2022). The IIS was particularly sensitive to temperature changes due to its relatively low ELA, low-gradient topography, and maritime climate (Norðdahl and Ingólfsson, 2015; Hannesdóttir *et al.*, 2015; Patton *et al.*, 2017; Andrés *et al.*, 2019). Thus, it may be a particularly appropriate case study of ice response to rapid temperature rise under future or even current climate warming scenarios, which is crucial given predicted glacier retreat, meltwater lake expansion, and hydrologic impacts on natural and human systems worldwide (Huss and Hock, 2018; Farinotti *et al.*, 2019; Shugar *et al.*, 2020; How *et al.*, 2021; Huggonet *et al.*, 2021).

FUTURE RESEARCH AGENDAS

Numerous research directions remain to reconstruct the Hvítá jökulhlaups and situate these events within early Holocene environmental change in Iceland. We highlight three worthwhile future lines of inquiry:

- Expand geomorphologic field mapping by: 1) surveying the eastern side of Bláfell to ground truth potential flood evidence identified in remote sensing imagery; and 2) exploring downstream of the Sandá channels and Hvítárgljúfur canyon, potentially with subsurface imaging, to search for flood deposits to help constrain flood routing, geomorphologic impact, and relative chronology.
- Reconstruct the location, volume, and stages of Glacial Lake Kjölur by mapping paleolake shoreline extent and elevation. This links meltwater source with downstream flood routes and impacts, helping to understand glacial lake evolution and flood recurrence interval and drainage dynamics.
- Model ice sheet position and evolution during the final phase of IIS retreat. Jökulhlaup geomorphol-

ogy and geochronology will help to calibrate ice sheet models and test output simulations, yielding insight into links between climate, ice behavior, and hydrologic response.

Acknowledgements

GHW completed this work while on a Fulbright Iceland-NSF Arctic Research Grant, a University of Texas-Austin Graduate Continuing Fellowship, and a University of Texas-Austin graduate research assistant position. Field work was supported by grants to GHW from the Leifur Eiríksson Foundation Fellowship, American-Scandinavian Foundation Fellowship, American Association of Geographers Dissertation Research Grant, Explorers Club Exploration Fund Grant, Geological Society of America Graduate Student Research Grant, and University of Texas-Austin Global Research Fellowship. We would like to thank Magnús Tumi Guðmundsson and Jón Örn Bjarnason for translating the Tómasson (1993) and Kjartansson (1964) articles, respectively, from Icelandic to English; and Joaquín M. C. Belart for assisting with elevation data. We also thank the Institute of Earth Sciences at the University of Iceland for hosting GHW during part of this project. Finally, GHW would like to thank the staff at Árbúðir hut in Kjölur for their hospitality and support during field campaigns. Insightful comments from Magnús Tumi Guðmundsson and an anonymous reviewer helped to improve this manuscript.

ÁGRIP

Jökulhlaup (Glacial outburst floods) hafa verið mikilvægur þáttur í landslagsmótun og umhverfisbreytingum á Ísöldinni (Quaternary). Á Íslandi er tíðni jökulhlaupa meiri en á öðrum stöðum á jörðinni, en flestar rannsóknir hafa beinst að jökulhlaupum sem eiga upptök sín undir jöklum vegna eldvirkni (subglacial volcanogenic floods). Umfangsmikil jarðfræðileg ummerki finnast meðfram farvegi Hvítár á suðvestanverðu landinu, sem benda til stórra jökulhlaupa á fyrri hluta nútíma (Holocene) frá jökulstífluðu lóni á Kili. Hingað til hefur einungis ein fræðigrein (Haukur Tómasson, 1993) verið rituð um þessi miklu flóð. Okkar rannsóknir byggja á kortlagningu landforma og fjarkönnun á ummerkjum jökulhlaupa meðfram farvegi Hvítár. Við rannsökuðum rofform og kerfi farvega í berggrunni, gljúfur og setmyndanir, svo sem stórgrýtisdreif og set í árfarvegum. Okkar niðurstöður eru settar fram með: 1) uppfærðu landmótunarkorti af ummerkjum jökulhlaupa í Hvítá; 2) endurgerð á farvegakerfi hlaupanna, landmótun þeirra, vatnafræði ásamt afstæðum aldursgreiningum og 3) nýjum kenningum um útbreiðslu og legu jökla og jökullóna. Ítarlegri túlkun á landformum sem mynduðust í flóðunum hefur leitt í ljós mun flóknara flæðimynstur í fjórum farvegakerfum með upptök hugsanlega á tveimur mismunandi stöðum. Endurreiknað hámarksrennsli flóðanna er metið á bilinu frá 10^2 upp í 10^5 m^3 s^{-1}. Á grundvelli landfræðilegra og vatnafræðilegra gagna er hægt að setja upp fjórar mismunandi sviðsmyndir á því hvernig flóðin áttu sér stað, en til að ákvarða fjölda flóða í hverjum farvegi þarf nákvæmari aldursgreiningar. Jökulhlaupin í Hvítá gefa skýra mynd af þeim miklu umhverfisbreytingum sem áttu sér stað í lok síðasta jökulskeiðs á Íslandi og varpa ljósi á áhrif stórra en sjaldgæfra jökulhlaupa á mótun landslags. Slík hamfarahlaup endurspegla umhverfisbreytingar fortíðar, en geta hugsanlega orðið í framtíðinni við áframhaldandi hlýnun á jöklasvæðum jarðar.

REFERENCES

Aðalgeirsdóttir, G., S. Guðmundsson, H. Björnsson, F. Pálsson, T. Jóhannesson, H. Hannesdóttir, S.P. Sigurðsson and E. Berthier 2011. Modelling the 20th and 21st century evolution of Hoffellsjökull glacier, SE-Vatnajökull, Iceland. *Cryosphere* 5, 961–975. https://doi.org/10.1029/2005JF000388

Aðalgeirsdóttir, G., E. Magnússon, F. Pálsson, T. Thorsteinsson, J.M.C. Belart, T. Jóhannesson, H. Hannesdóttir, O. Sigurðsson, A. Gunnarsson, B. Einarsson, E. Berthier, L.S. Schmidt, H.H. Haraldsson and H. Björnsson 2020. Glacier Changes in Iceland from ∼1890 to 2019. *Front. Earth Sci.* 8, 523646. http://doi.org/10.3389/feart.2020.523646

Amidon, W.H. and A.C. Clark 2015. Interaction of outburst floods with basaltic aquifers on the Snake River plain: Implications for Martian canyons. *Bull. Geol. Soc. Am.* 127, 688–701. https://doi.org/10.1130/-B31141.1

Anderson, S. P., J. S. Walder, R. S. Anderson, E. R. Kraal, M. Cunico, A. G. Fountain and D. C. Trabant 2003. Integrated hydrologic and hydrochemical observations of Hidden Creek Lake jökulhlaups, Kennicott Glacier, Alaska. *J. Geophys. Res. Earth Surf.* 108, 6003. https://doi.org/10.1029/2002jf000004

Andrés, N., D. Palacios, Þ. Sæmundsson, S. Brynjólfsson and J. M. Fernández-Fernández 2019. The rapid deglaciation of the Skagafjörður fjord, northern Iceland. *Boreas* 48, 92–106. https://doi.org/10.1111/-bor.12341

Áskelsson, J. 1946. A contribution to the geology of the Kerlingarfjöll. *Acta Nat. Isl.* 1(2), 3–15.

Axford, Y., A. de Vernal and E. C. Osterberg 2021. Past warmth and its impacts during the Holocene Thermal Maximum in Greenland. *Annu. Rev. Earth Planet. Sci.* 49, 279–307. https://doi.org/10.1146/annurev-earth-081420-063858

Baker, V. R. 1973. *Paleohydrology and sedimentology of Lake Missoula flooding in eastern Washington.* Special Paper 144. Geological Society of America, Boulder, CO, 79 pp. https://doi.org/10.1130/SPE144-p1

Baker, V. R. 1978. Large-scale erosional and depositional features of the Channeled Scabland. In: Baker, V. R. (ed.) 1981. *Catastrophic Flooding: The Origin of the Channeled Scabland.* Dowden, Hutchinson and Ross, Stroudsburg, PA, 276–310.

Baker, V. R. 2009. Channeled Scabland morphology. In: Burr, D.M., P.A. Carling and V. R. Baker (eds.). *Megaflooding on Earth and Mars.* Cambridge University Press, Cambridge, U.K., 65–77. https://doi.org/-10.1017/CBO9780511635632.005

Baker, V. R. 2013. Global late Quaternary fluvial paleohydrology: with special emphasis on paleofloods and megafloods. In: Schroder, J. and E. Wohl (eds.). *Treatise on Geomorphology 9, Fluvial Geomorphology.* Academic Press, San Diego, CA, 511–527. https://doi.org/10.1016/B978-0-12-374739-6.00252-9

Baynes, E. R. C., M. Attal, A. J. Dugmore, L. A. Kirstein and K. A. Whaler 2015a. Catastrophic impact of extreme flood events on the morphology and evolution of the lower Jökulsá á Fjöllum (northeast Iceland) during the Holocene. *Geomorphology* 250, 422–436. https://doi.org/10.1016/j.geomorph.2015.05.009

Baynes, E. R. C., M. Attal, S. Niedermann, L.A. Kirstein, A.J. Dugmore and M. Naylor 2015b. Erosion during extreme flood events dominates Holocene canyon evolution in northeast Iceland. *Proc. Natl. Acad. Sci.* U.S.A. 112, 2355–2360. https://doi.org/-10.1073/pnas.141544311

Benito, G. 1997. Energy expenditure and geomorphic work of the cataclysmic Missoula flooding in the Columbia River Gorge, USA. *Earth Surf. Process. Landf.* 22, 457–472. https://doi.org/-10.1002/(SICI)1096-9837(199705)22:5<457::AID-ESP762>3.0.CO;2-Y

Benito, G. and V. R. Thorndycraft 2020. Catastrophic glacial-lake outburst flooding of the Patagonian Ice Sheet. *Earth-Sci. Rev.* 200, 102996. https://doi.org/-10.1016/j.earscirev.2019.102996

Benito, G., V. R. Thorndycraft, A. Medialdea, M. J. Machado, C. Sancho and A. Dussaillant 2021. Declining discharge of glacier outburst floods through the Holocene in central Patagonia. *Quat. Sci. Rev.* 256, 106810. https://doi.org/10.1016/j.quascirev.-2021.106810

Benn, D. I. and D. J. A. Evans 2010. *Glaciers and Glaciation* (Second ed.). Hodder Education, London, 802 pp.

Bennett, M. R. and N. F. Glasser 2009. *Glacial Geology: Ice Sheets and Landforms* (Second ed.). Wiley-Blackwell, Chichester, U.K., 385 pp.

Björnsson, H. 2002. Subglacial lakes and jökulhlaups in Iceland. *Glob. Planet. Change* 35, 255–271. https://doi.org/10.1016/S0921-8181(02)00130-3

Bretz, J. H. 1923. The Channeled Scablands of the Columbia Plateau. *J. Geol.* 31, 617–649. https://doi.org/-10.1086/623053

Brovkin, V., E. Brook, J. W. Williams, S. Bathiany, T. M. Lenton, M. Barton, R. M. DeConto, J. F. Donges, A. Ganopolski, J. McManus, S. Praetorius, A. de Vernal, A. Abe-Ouchi, H. Cheng, M. Claussen, M. Crucifix, G. Gallopín, V. Iglesias, D. S. Kaufman, T. Kleinen, F. Lambert, S. van der Leeuw, H. Liddy, M.-F. Loutre, D. McGee, K. Rehfeld, R. Rhodes, A. W. R. Seddon, M. H. Trauth, L. Vanderveken and Z. Yu 2021. Past abrupt changes, tipping points and cascading impacts in the Earth system. *Nat. Geosci.* 1, 5540–558. https://doi.org/10.1038/s41561-021-00790-5

Carling, P. A., J. Herget, J. K. Lanz, K. Richardson and A. Pacifici 2009. Channel-scale erosional bedforms in bedrock and in loose granular material: character, processes and implications. In: Burr, D.M., P.A. Carling and V.R. Baker (eds.). *Megaflooding on Earth and Mars.* Cambridge University Press, Cambridge, U.K., 13–32. http://doi.org/10.1017/CBO9780511635632.002

Carling, P. A. 2013. Freshwater megaflood sedimentation: What can we learn about generic processes? *Earth-Sci. Rev.* 125, 87–113. https://doi.org/10.1016/-j.earscirev.2013.06.002

Carrivick, J. L. 2007. Hydrodynamics and geomorphic work of jökulhlaups (glacial outburst floods) from Kverkfjöll volcano, Iceland. *Hydro. Process.* 21, 725–740. https://doi.org/10.1002/hyp.6248

Carrivick, J. L. and F. S. Tweed 2013. Proglacial lakes: character, behaviour and geological importance. *Quat. Sci. Rev.* 78, 34–52. https://doi.org/-10.1016/j.quascirev.2013.07.028

Carrivick, J. L. and F. S. Tweed 2016. A global assessment of the societal impacts of glacier outburst floods. *Glob. and Planet. Change* 144, 1–16. https://doi.org/-10.1016/j. gloplacha.2016.07.001

Carrivick, J. L. and F. S. Tweed 2019. A review of glacier outburst floods in Iceland and Greenland with a megafloods perspective. *Earth-Sci. Rev.* 196, 102876. https://doi.org/10.1016/j.earscirev.2019.102876

Carrivick, J. L., A. J. Russell and F. S. Tweed 2004a. Geomorphological evidence for jökulhlaups from Kverkfjöll volcano, Iceland. *Geomorphology* 63, 81–102. https://doi.org/ 10.1016/j.geomorph.2004.03.006

Carrivick, J. L., A. J. Russell, F. S. Tweed and D. Twigg 2004b. Palaeohydrology and sedimentary impacts of jökulhlaups from Kverkfjöll, Iceland. *Sediment. Geol.* 172, 19–40. https://doi.org/-10.1016/j.sedgeo.2004.07.005

Carrivick, J. L., F. S. Tweed, J. L. Sutherland and J. Mallalieu 2020. Toward numerical modeling of interactions between ice-marginal proglacial lakes and glaciers. *Front. Earth Sci.* 8, 577068. https://doi.org/-10.3389/feart.2020.577068

Chow, V. T. 1959. *Open-channel hydraulics.* McGraw-Hill, Tokyo. 679 pp.

Clarke, G. K. C., D. W. Leverington, J. T. Teller and A. S. Dyke 2004. Paleohydraulics of the last outburst flood from glacial Lake Agassiz and the 8200 BP cold event. *Quat. Sci. Rev.* 23, 389–407. https://doi.org/-10.1016/j.quascirev.2003.06.004

Cook, K. L., C. Andermann, F. Gimbert, B. R. Adhikari and N. Hovius 2018. Glacial lake outburst floods as drivers of fluvial erosion in the Himalaya. *Science* 362, 53–57. https://doi.org/10.1126/science.aat4981

Dunning, S. A., A. R. G. Large, A. J. Russell, M. J. Roberts, R. Duller, J. Woodward, A. S. Mériaux, F. S. Tweed and M. Lim 2013. The role of multiple glacier outburst floods in proglacial landscape evolution: The 2010 Eyjafjallajökull eruption, Iceland. *Geology* 41, 1123–1126. https://doi.org/10.1130/G34665.1

Dussaillant, A., G. Benito, W. Buytaert, P. Carling, C. Meier and F. Espinoza 2010. Repeated glacial-lake outburst floods in Patagonia: an increasing hazard? *Nat. Hazards* 54, 469–481. https://doi.org/-10.1007/s11069-009-9479-8

Eason, D. E., J. M. Sinton, K. Grönvold and M. D. Kurz 2015. Effects of deglaciation on the petrology and eruptive history of the Western Volcanic Zone, Iceland. *Bull. Volcanol.* 77, 47. https://doi.org/-10.1007/s00445-015-0916-0

Evans, S. G. and J. J. Clague 1994. Recent climatic change and catastrophic geomorphic processes in mountain environments. *Geomorphology* 10, 107–128. https://doi.org/10.1016/0169-555X(94)90011-6

Farinotti, D., V. Round, M. Huss, L. Compagno and H. Zekollari 2019. Large hydropower and water-storage potential in future glacier-free basins. *Nature* 575, 341–344. https://doi.org/10.1038/s41586-019-1740-z

Fisher, T. G. 2020. Megaflooding associated with glacial Lake Agassiz. *Earth-Sci. Rev.* 201, 102974. https://doi.org/10.1016/j.earscirev.2019.102974

Garcia-Castellanos, D. and J. E. O'Connor 2018. Outburst floods provide erodability estimates consistent with long-term landscape evolution. *Sci. Rep.* 8, 10573. https://doi.org/10.1038/s41598-018-28981-y

Geirsdóttir, Á., G. H. Miller, Y. Axford and S. Ólafsdóttir 2009. Holocene and latest Pleistocene climate and glacier fluctuations in Iceland. *Quat. Sci. Rev.* 28, 2107–2118. https://doi.org/10.1016/-j.quascirev.2009.03.013

Glasser, N. F. and M. R. Bennett 2004. Glacial erosional landforms: origins and significance for palaeoglaciology. *Prog. Phys. Geogr.* 28, 43–75. https://doi.org/-10.1191/0309133304pp401ra

Grinsted, A., C. S. Hvidberg, N. Campos and D. Dahl-Jensen 2017. Periodic outburst floods from an ice-dammed lake in East Greenland. *Sci. Rep.* 7, 9966. https://doi.org/10.1038/s41598-017-07960-9

Guðmundsson, S., H. Björnsson, F. Pálsson, E. Magnússon, Þ. Sæmundsson and T. Jóhannesson 2019. Terminus lakes on the south side of Vatnajökull ice cap, SE-Iceland. *Jökull* 69, 1–34. https://doi.org/-10.33799/jokull2019.69.001

Halldorsson, S. A., N. Oskarsson, K. Gronvold, G. Sigurdsson, G. Sverrisdottir and S. Steinthorsson 2008. Isotopic-heterogeneity of the Thjorsa lava-Implications for mantle sources and crustal processes within the Eastern Rift Zone, Iceland. *Chem. Geol.* 255, 305–316. https://doi.org/-10.1016/j.chemgeo.2008.06.050

Hannesdóttir, H. 2006. *Reconstructing environmental change in South Iceland during the last 12,000 cal. yr based on sedimentological and seismostratigraphical studies in lake Hestvatn.* MSc thesis, University of Iceland, 143 pp.

Hannesdóttir, H., A. Geirsdóttir, G. H. Miller, W. Manley and N. Wattrus 2009. Deglacial and Holocene sediment distribution in Hestvatn, South Iceland, derived from a seismic and multibeam survey. *Jökull* 59, 67–88.

Hannesdóttir, H., O. Sigurðsson, R. Þrastarson, S. Guðmundsson, J. Belart, F. Pálsson, E. Magnússon, S. Víkingsson and T. Jóhannesson 2020. A national glacier inventory and variations in glacier extent in Iceland from the Little Ice Age maximum to 2019. *Jökull* 70, 1–34. https://doi.org/-10.33799/jokull2020.70.001

Harrison, S., J. S. Kargel, C. Huggel, J. Reynolds, D. H. Shugar, R. A. Betts, A. Emmer, N. Glasser, U. K. Haritashya, J. Klimeš, L. Reinhardt, Y. Schaub, A. Wiltshire, D. Regmi and V. Vilímek 2018. Climate change and the global pattern of moraine-dammed glacial lake outburst floods. *Cryosphere* 12, 1195–1209. https://doi.org/10.5194/tc-12-1195-2018

Herget, J. 2005. *Reconstruction of Pleistocene ice-dammed lake outburst floods in the Altai Mountains, Siberia.* Special Paper 386. Geological Society of America, Boulder, CO, 118 pp. https://doi.org/-10.1130/SPE386

Hjartarson, A. 1988. Þjórsárhraunið mikla, stærsta nútímahraun jarðar. *Náttúrufræðingurinn* 58, 1–16.

How, P., A. Messerli, E. Mätzler, M. Santoro, A. Wiesmann, R. Caduff, K. Langley, M. H. Bojesen, F. Paul, A. Kääb and J. L. Carrivick 2021. Greenland-wide inventory of ice marginal lakes using a multi-method approach. *Sci. Rep.* 11, 4481. https://doi.org/-10.1038/s41598-021-83509-1

Hubbard, A., D. Sugden, A. Dugmore, H. Norðdahl and H. G. Pétursson 2006. A modelling insight into the Icelandic Last Glacial Maximum ice sheet. *Quat. Sci. Rev.* 25, 2283–2296. https://doi.org/-10.1016/j.quascirev.2006.04.001

Hugonnet, R., R. McNabb, E. Berthier, B. Menounos, C. Nuth, L. Girod, D. Farinotti, M. Huss, I. Dussaillant, F. Brun and A. Kääb 2021. Accelerated global glacier mass loss in the early twenty-first century. *Nature* 592, 726–731. https://doi.org/10.1038/s41586-021-03436-z

Huss, M. and R. Hock 2018. Global-scale hydrological response to future glacier mass loss. *Nat. Clim. Chang.* 8, 135–140. https://doi.org/10.1038/s41558-017-0049-x

Ingólfsson, Ó., H. Norðdahl and A. Schomacker 2010. Deglaciation and Holocene glacial history of Iceland. In: Schomacker, A., J. Krüger and K. H. Kjær (eds.). *The Mýrdalsjökull Ice Cap, Iceland: Glacial Processes, Sediments and Landforms on an Active Volcano.* Elsevier, Amsterdam, 51–68.

ÍslandsDEM, 2021. Landmælingar Íslands. Accessed from https://gatt.lmi.is/geonetwork/srv/api/records/e6712430-a63c-4ae5-9158-c89d16da6361.

Jacquet, J., S. W. McCoy, D. McGrath, D. A. Nimick, M. Fahey, J. O'kuinghttons, B. A. Friesen and J. Leidich 2017. Hydrologic and geomorphic changes resulting from episodic glacial lake outburst floods: Rio Colonia, Patagonia, Chile. *Geophys. Res. Lett.* 44, 854–864. https://doi.org/10.1002/2016GL071374

Jóhannesson, H. and K. Sæmundsson 2009. *Geological Map of Iceland. 1:600 000. Tectonics.* Icelandic Museum of Natural History and Icelandic Geodetic Survey, Reykjavík (First ed.).

Kaldal, I. and S. Víkingsson 1990. Early Holocene deglaciation in Central Iceland. *Jökull* 40, 51–66.

Kjartansson, G. 1964. Ísaldarlok og eldfjöll á Kili. *Náttúrufræðingurinn* 34, 9–38.

Kjartansson, G. 1967. The Steinsholtshlaup, central-south Iceland on January 15th, 1967. *Jökull* 17, 249–262.

Komatsu, G., V. R. Baker, S. G. Arzhannikov, R. Gallagher, A. V. Arzhannikova, A. Murana and T. Oguchi 2016. Catastrophic flooding, palaeolakes, and late Quaternary drainage reorganization in northern Eurasia. Int. Geol. Rev. 58, 1693–1722. https://doi.org/-10.1080/00206814.2015.1048314

Lamb, M. P. and W. E. Dietrich 2009. The persistence of waterfalls in fractured rock. Bull. Geol. Soc. Am. 121, 1123–1134. https://doi.org/10.1130/B26482.1

Lamb, M. P., W. E. Dietrich, S. M. Aciego, D. J. DePaolo and M. Manga 2008. Formation of Box Canyon, Idaho, by megaflood: Implications for seepage erosion on Earth and Mars. *Science* 320, 1067–1070. https://doi.org/10.1126/science.1156630

Lamb, M. P., B. H. Mackey and K. A. Farley 2014. Amphitheater-headed canyons formed by megaflooding at Malad Gorge, Idaho. Proc. Natl. Acad. Sci. U.S.A. 111, 57–62. https://doi.org/-10.1073/pnas.131225111

Landmælingar Íslands (National Land Survey of Iceland). Aerial photo gallery. Accessed from https://www.lmi.is/is/vefsjar/korta-og-loftmynda-sofn/loftmyndasafn

Larsen, I. J. and M. P. Lamb 2016. Progressive incision of the Channeled Scablands by outburst floods. *Nature* 538, 229–232. https://doi.org/10.1038/nature19817

Larsen, D. J., G. H. Miller, Á. Geirsdóttir and S. Ólafsdóttir 2012. Non-linear Holocene climate evolution in the North Atlantic: a high-resolution, multi-proxy record of glacier activity and environmental change from Hvítárvatn, central Iceland. *Quat. Sci. Rev.* 39, 14–25. https://doi.org/-10.1016/j.quascirev.2012.02.006

Lehnigk, K. E. and I. J. Larsen 2022. Pleistocene megaflood discharge in Grand Coulee, Channeled Scabland, USA. *J. Geophys. Res. Earth Surf.* 127, e2021JF006135. https://doi.org/10.1029/2021JF-006135

Licciardi, J. M., M. D. Kurz and J. M. Curtice 2007. Glacial and volcanic history of Icelandic table mountains from cosmogenic 3He exposure ages. *Quat. Sci. Rev.* 26, 1529–1546. https://doi.org/10.1016/-j.quascirev.2007.02.016

Loftmyndir ehf. *Map viewer.* Accessed from https://map.is.

Maclennan, J., M. Jull, D. Mckenzie, L. Slater and K. Grönvold 2002. The link between volcanism and deglaciation in Iceland. *Geochem. Geophys. Geosyst.* 3(11), 1062. https://doi.org/10.1029/2001GC000282

Magnússon, E., F. Pálsson, M. T. Gudmundsson, T. Högnadóttir, C. Rossi, T. Thorsteinsson, B. G. Ófeigsson, E. Sturkell and T. Jóhannesson 2021. Development of a subglacial lake monitored with radio-echo sounding: case study from the eastern Skaftá cauldron in the Vatnajökull ice cap, Iceland. *Cryosphere* 15, 3731–3749. https://doi.org/10.5194/tc-15-3731-2021

Maizels, J. 1997. Jökulhlaup deposits in proglacial areas. *Quat. Sci. Rev.* 16, 793–819. https://doi.org/-10.1016/S0277-3791(97)00023-1

Marren, P. M. 2002. Criteria for distinguishing high magnitude flood events in the proglacial fluvial sedimentary record. In: Snorrason, A., H. P. Finnsdóttir and M. Moss (eds.). *The Extremes of the Extremes: Extraordinary Floods.* International Association of Hydrological Sciences Publication 271, proceedings of a symposium in Reykjavík, Iceland. IAHS Press, Wallingford, Oxfordshire, U.K., 237–241.

Marren, P. M. 2005. Magnitude and frequency in proglacial rivers: a geomorphological and sedimentological perspective. *Earth-Sci. Rev.* 70, 203–251. https://doi.org/10.1016/j.earscirev.2004.12.002

Marren, P. M. and M. Schuh 2009. Criteria for identifying jökulhlaup deposits in the sedimentary record. In: Burr, D. M., P. A. Carling and V. R. Baker (eds.). *Megaflooding on Earth and Mars.* Cambridge University Press, Cambridge, U.K., 225–242.

Marren, P. M., A. J. Russell and E. L. Rushmer 2009. Sedimentology of a sandur formed by multiple jökulhlaups, Kverkfjöll, Iceland. *Sediment. Geol.* 213, 77–88. https://doi.org/10.1016/j.sedgeo.2008.11.006

Meara, R. H. H., Th. Thordarson, N. J. G. Pearce, C. Hayward and G. Larsen 2020. A catalogue of major and trace element data for Icelandic Holocene silicic tephra layers. *J. Quat. Sci.* 35, 122–142. https://doi.org/10.1002/jqs.3173

Norðdahl, H. and Ó. Ingólfsson 2015. Collapse of the Icelandic ice sheet controlled by sea-level rise? *Arktos* 1(13). https://doi.org/10.1007/s41063-015-0020-x

Norðdahl, H., O. Ingólfsson, H. G. Pétursson and M. Hallsdóttir 2008. Late Weichselian and Holocene environmental history of Iceland. *Jökull* 58, 343–364.

O'Connor, J. E. 1993. *Hydrology, hydraulics, and geomorphology of the Bonneville flood.* Special Paper 274. Geological Society of America, Boulder, CO, 83 pp. https://doi.org/10.1130/SPE274-p1.

O'Connor, J. E., V. R. Baker, R. B. Waitt, L. N. Smith, C. M. Cannon, D. L. George and R. P. Denlinger 2020. The Missoula and Bonneville floods – A review of ice-age megafloods in the Columbia River basin. *Earth-Sci. Rev.* 208, 103181. https://doi.org/-10.1016/j.earscirev.2020.103181

Patton, H., A. Hubbard, T. Bradwell and A. Schomacker 2017. The configuration, sensitivity and rapid retreat of the Late Weichselian Icelandic ice sheet. *Earth-Sci. Rev.* 166, 223–245. https://doi.org/-10.1016/j.earscirev.2017.02.001

Pico, T., S. R. David, I. J. Larsen, A. C. Mix, K. Lehnigk and M. P. Lamb 2022. Glacial isostatic adjustment directed incision of the Channeled Scabland by Ice Age megafloods. *Proc. Natl. Acad. Sci.* U.S.A. 119(8), e2109502119. https://doi.org/-10.1073/pnas.2109502119

Piret, L., S. Bertrand, N. Nguyen, J. Hawkings, C. Rodrigo and J. Wadham 2022. Long-lasting impacts of a 20th century glacial lake outburst flood on a Patagonian fjord-river system (Pascua River). *Geomorphology* 399, 108080. https://doi.org/-10.1016/j.geomorph.2021.108080

Porter, C., P. Morin, I. Howat, M.-J. Noh, B. Bates, K. Peterman, S. Keesey, M. Schlenk, J. Gardiner, K. Tomko, M. Willis, C. Kelleher, M. Cloutier, E. Husby, S. Foga, H. Nakamura, M. Platson, M. Wethington, C. Williamson, G. Bauer, J. Enos, G. Arnold, W. Kramer, P. Becker, A. Doshi, C. D'Souza, P. Cummens, F. Laurier and M. Bojesen 2018. *ArcticDEM. Harvard Dataverse, V1*. https://doi.org/10.7910/DVN/OHHUKH.

Praetorius, S. K., A. Condron, A. C. Mix, M. H. Walczak, J. L. McKay, J. Du 2020. The role of Northeast Pacific meltwater events in deglacial climate change. *Sci. Adv.* 6, eaay2915. https://doi.org/10.1126/sciadv.aay2915

Rathburn, S. L. 1993. Pleistocene cataclysmic flooding along the Big Lost River, east central Idaho. *Geomorphology* 8, 305–319. https://doi.org/10.1016/0169-555X(93)90026-X

Regnéll, C., J. Mangerud and J. I. Svendsen 2019. Tracing the last remnants of the Scandinavian Ice Sheet: Ice-dammed lakes and a catastrophic outburst flood in northern Sweden. *Quat. Sci. Rev.* 221, 105862. https://doi.org/10.1016/j.quascirev.2019.105862

Rick, B., D. McGrath, W. Armstrong and S. W. McCoy 2022. Dam type and lake location characterize ice-marginal lake area change in Alaska and NW Canada between 1984 and 2019. *Cryosphere* 16, 297–314. https://doi.org/10.5194/tc-16-297-2022

Roberts, M. J. 2005. Jökulhlaups: A reassessment of floodwater flow through glaciers. *Rev. Geophys.* 43, RG1002. https://doi.org/10.1029/2003RG000147

Roberts, M. J., F. Pálsson, M. T. Gudmundsson, H. Björnsson and F. S. Tweed 2005. Ice-water interactions during floods from Grænalón glacier-dammed lake, Iceland. *Ann. Glaciol.* 40, 133–138. https://doi.org/-10.3189/172756405781813771

Rushmer, E. L. 2006. Sedimentological and geomorphological impacts of the jökulhlaup (glacial outburst flood) in January 2002 at Kverkfjöll, northern Iceland. *Geogr. Ann.* 88 A(1), 43–53. https://doi.org/-10.1111/j.0435-3676.2006.00282.x

Russell, A. J., J. L. Carrivick, T. Ingeman-Nielsen, J. C. Yde and M. Williams 2011. A new cycle of jökulhlaups at Russell Glacier, Kangerlussuaq, West Greenland. *J. Glaciol.* 57, 238–246. https://doi.org/10.3189/002214311796405997

Russell, A. J., H. Fay, P. M. Marren, F. S. Tweed and Ó. Knudsen 2005. Icelandic jökulhlaup impacts. In: Caseldine, C., A. Russell, J. Harðardóttir and Ó. Knudsen (eds.). *Iceland – Modern Processes and Past Environments.* Elsevier, Amsterdam, 153–203.

Russell, A. J., M. J. Roberts, H. Fay, P. M. Marren, N. J. Cassidy, F. S. Tweed and T. Harris 2006. Icelandic jökulhlaup impacts: Implications for ice-sheet hydrology, sediment transfer and geomorphology. *Geomorphology* 75, 33–64. https://doi.org/-10.1016/j.geomorph.2005.05.018

Shugar, D. H., A. Burr, U. K. Haritashya, J. S. Kargel, C. S. Watson, M. C. Kennedy, A. R. Bevington, R. A. Betts, S. Harrison and K. Strattman 2020. Rapid worldwide growth of glacial lakes since 1990. *Nat. Clim. Chang.* 10, 939–945. https://doi.org/10.1038/s41558-020-0855-4

Sinton, J., K. Grönvold and K. Sæmundsson 2005. Postglacial eruptive history of the Western Volcanic Zone, Iceland. *Geochem. Geophys. Geosyst.* 6, Q12009. https://doi.org/10.1029/2005GC001021

Stokes, M., J. S. Griffiths and A. Mather 2012. Palaeoflood estimates of Pleistocene coarse grained river terrace landforms (Río Almanzora, SE Spain). *Geomorphology* 149–150, 11–26. https://doi.org/10.1016/j.geomorph.2012.01.007

Stucky de Quay, G., G. G. Roberts, D. H. Rood and V. M. Fernandes 2019. Holocene uplift and rapid fluvial erosion of Iceland: A record of post-glacial landscape evolution. *Earth. Planet. Sci. Lett.* 505, 118–130. https://doi.org/10.1016/j.epsl.2018.10.026

Sutherland, J. L., J. L. Carrivick, N. Gandy, J. Shulmeister, D. J. Quincey and S. L. Cornford 2020. Proglacial lakes control glacier geometry and behavior during recession. *Geophys. Res. Lett.* 47, e2020GL088865. https://doi.org/10.1029/2020GL088865

Thorarinsson, S. 1939. The ice dammed lakes of Iceland with particular reference to their values as indicators of glacier oscillations. *Geogr. Ann.* 21, 216–242.

Thordarson, T. and A. Höskuldsson 2002. *Iceland.* Dunedin Academic Press, 224 pp.

Þorsteinsson, Þ., K. G. Eyþórsdóttir, E. H. Jensen, I. Jónsdóttir, F. Pálsson, G. Sigurðsson, A. Gunnarsson, H. S. Pálsson, R. H. Þrastarson, O. Sigurðsson, T. Jóhannesson and M. Roberts 2021. *Jökulhlaup úr Hafrafellslóni við Langjökul.* Veðurstofa Íslands, Report VÍ 2021-001, 33 pp.

Tómasson, H. 1973. Hamfarahlaup í Jökulsá á Fjöllum. *Náttúrufræðingurinn* 43, 12–34.

Tómasson, H. 1993. Jökulstífluð vötn á Kili og hamfarahlaup í Hvítá í Árnessýslu. *Náttúrufræðingurinn* 62, 77–98.

Tómasson, H. 1996. The jökulhlaup from Katla in 1918. *Ann. Glaciol.* 22, 249–254. https://doi.org/10.3189/-1996AoG22-1-249-254.

Tómasson, H. 2002. Catastrophic floods in Iceland. In: Snorrason, A., H. P. Finnsdóttir and M. Moss (eds.). *The Extremes of the Extremes: Extraordinary Floods.* International Association of Hydrological Sciences Publication 271, proceedings of a symposium in Reykjavík, Iceland. IAHS Press, Wallingford, Oxfordshire, U.K., 121–126.

Tweed, F. S. and A. J. Russell 1999. Controls on the formation and sudden drainage of glacier-impounded lakes: implications for jökulhlaup characteristics. *Prog. Phys. Geogr.* 23(1), 79–110. https://doi.org/-10.1177/030913339902300104

Van der Bilt, W. G. M., I. D. Barr, S. M. P. Berben, R. Hennekam, T. Lane, K. Adamson and J. Bakke 2021. Late Holocene canyon-carving floods in northern Iceland were smaller than previously reported. *Commun. Earth Environ.* 2(86). https://doi.org/10.1038/s43247-021-00152-4

Van Vliet-Lanoë, B., O. Knudsen, A. Guðmundsson, H. Guillou, G. Chazot, J. Langlade, C. Liorzou and P. Nonnotte 2020. Volcanoes and climate: the triggering of preboreal Jökulhlaups in Iceland. *Int. J. Earth Sci.* 109, 847–876. https://doi.org/10.1007/s00531-020-01833-9

Ward, A. D. and S. W. Trimble 2004. *Environmental Hydrology.* 2nd ed. CRC Press, Boca Raton, FL. 475 pp.

Wells, G. H., A. Dugmore, T. Beach, Þ. Sæmundsson, E. R. C. Baynes and S. Luzzadder-Beach 2022. Reconstructing glacial outburst floods (jökulhlaups) from geomorphology: interpretive challenges, solutions, and an enhanced conceptual framework. *Prog. Phys. Geogr.* 46(3), 398–421. https://doi.org/-10.1177/03091333211065001

Whipple, K. X., G. S. Hancock and R. S. Anderson 2000. River incision into bedrock: Mechanics and relative efficacy of plucking, abrasion, and cavitation. *Bull. Geol. Soc. Am.* 112, 490–503. https://doi.org/10.1130/0016-7606(2000)112<490:RIIBMA>2.0.CO;2